

## **Response to Referee #1:**

We acknowledge the referee's very helpful and detailed review and encouragement. We take the suggestions to reduce redundancy between model description and discussions. The section 2 is now more concise and the detailed phenology description is moved to Supplementary materials. Previous discussions on resource allocation mechanisms, i.e. sections 5.2 and 5.3 are removed and the subsections are condensed to one section. We revised the full manuscript and largely reduced its size (from 14,000 to 10,000 words). The title is also changed to indicate the new sub-model CLM-Palm.

This paper focuses on the model development of CLM-Palm including its sub-canopy structure and phenology and allocation functions, which are the bases for future application to simulate the effects of forest to oil palm conversion on carbon, water and energy fluxes. We indicate the idea of model application at the end of discussion. Two following studies are being conducted in this regard. Due to limited space in this paper, we only show model development and validations against LAI, yield and NPP here.

In this revision, we recalibrated the model with new oil palm leaf  $C:N$  ratio measured recently and with slightly corrected harvest data obtained from the PTPN-VI plantation. We also treat the validation plots in Harapan and Bukit differently in respect of N fertilization. In the last version all the 8 plots were simulated with the same fertilization scheme like the industrial plantation PTPN-VI but actually the smallholder plots used much less fertilizer and the Bukit plots were not really fertilized in 2013 and 2014 (see Lines 297-306). New simulation results with two levels of fertilization (regular vs. reduced) significantly improve the modelled site-to-site variability in LAI and yield (see new Fig. 9 and 10), which matches closely with field data. We also add validation with NPP data measured from the 8 plots. Overall we try to demonstrate the ability of CLM-Palm to sufficiently represent the region-wide variability in oil palm NPP and yield driven by nutrient input and plantation age in Jambi, Sumatra.

(The line numbers all refer to the revised clean-version manuscript.)

## **Answers to specific comments:**

Comment 1: P3 You should be more clear the concept of PFT and sub-canopy structure in the abstract for attracting many readers.

Answer 1: We now add the name "CLM-Palm" in both the title and abstract so that the concept of PFT and sub-canopy structure is part of the new model. A PFT is usually not meant for only one species but for a group of species with shared functional traits and processes. CLM-Palm model is thus applicable for a PFT including oil palm as well as other palm species. The abstract is revised: "...we develop a new perennial crop sub-model CLM-Palm for simulating a palm plant functional type (PFT) within the framework of the Community Land Model (CLM4.5). CLM-Palm is tested here on oil palm only but is meant of generic interest for other palm crops (e.g. coconut)..." (Lines 20-28).

Comment 2: P5 L1-2 Why the models are not meant for studying carbon, water, and energy exchanges? It is hard to understand difference between yours and previous studies, here.

Answer 2: The agricultural models such as OPSIM, ECOPALM, APSIM-Oil Palm and PALMSIM are specialized for simulating the growth and yield of oil palm but they do not represent the full biophysical and biogeochemical cycles as a land surface model does. Their time steps are usually coarse (daily or monthly) and growth may not be constrained by photosynthesis supply. Land surface models such as CLM simulate energy, water and material cycling in a prognostic manner and at finer time steps (e.g. half-hourly). They also have strict check for energy and material balances. A land surface model is also meant to be coupled to climate models by providing land-to-atmosphere energy, water and carbon fluxes so that the feedbacks of terrestrial biosphere to climate can be simulated in coupled earth system model. Our CLM-Palm model is thus developed in the CLM framework, so that it combines the abilities of an agricultural model and a land surface model, which allows us to simulate climatic effects of the oil palm system in the next steps. We stated this in the discussions. (Lines 66-70 and Lines 559-561)

Comment 3: P6 L12 land-atmosphere fluxes of what?

Answer 3: land-to-atmosphere energy, water and carbon fluxes. We revised the sentence (Lines 96-97).

Comment 4: P6 L17 “Structure” means sub-model?

Answer 4: Yes, “structure” refers to the oil palm sub-model. It also refers to the sub-canopy vegetation structure and dimension that consider each phytomer as a simulation unit. “Structure” is modified to “CLM-Palm sub-model” (Lines 102-103) and we also give the model name “CLM-Palm” in the title.

Comment 5: P6 L17 simulating “oil palm plantation” of what? Growth and yields and anything else?

Answer 5: As the answer to comment 2, we simulate the growth and yield as well as fluxes of energy, water and carbon between the plantation land surface and atmosphere with 30-min time step. We revised this sentence to “In this context, we develop a new CLM-Palm sub-model for simulating the growth, yield, and energy and material cycling of oil palm within the framework of CLM4.5.” (Lines 102-103)

Comment 6: P10 L18 You showed “air temperature is the key variable or clock for the phenology”. That sounds reasonable in temperate regions. Is it applicable in tropical regions? How about moisture (such as dry and wet seasons)?

Answer 6: We agree that soil moisture or drought stress will act as key variable for oil palm growth and yield. CLM does include soil moisture in the photosynthesis-stomatal conductance module (see Fig. 2 model diagram) so that the effects of wet and dry season on assimilates supply are simulated. The effects pass to the carbon and nitrogen allocation module, which controls growth rate and yield. This process is operational in the CLM-Palm model as well.

On the other hand, the phenology subroutine relies on GDD (growing-degree days; accumulated temperature) to measure the length of phenological phases as typical for many phenological models. The original CLM model indeed includes soil moisture as a clock for the phenology of stress-deciduous PFTs, but only to initiate leaf litter-fall during severe drought. Oil palm, however, is an evergreen crop and does not shed leaves in dry seasons. Therefore, such a mechanism was not included. There might be effects of water stress on the timing of fruit initiation and maturity but the specific controls on these phenology steps are not sufficiently known to allow developing an appropriate function. That is why the CLM model only uses GDD as the clock for all the phenological phases of annual crop PFTs (e.g. wheat, corn). GDD is also useful in CLM-Palm to measure the thermal lengths of phenological periods, although air temperature has not much variation in the tropical regions.

In order to avoid confusion of the role of soil moisture in the CLM model (photosynthesis-stomatal conductance versus phenology), we simplify the sentence to: “All phytomers are assumed to follow the same phenological steps, where the thermal length for each phase is measured by growing degree-days (GDD; White et al., 1997)”. (Lines 159-160)

Comment 7: P10 L26 It is hard to understand concept of PFT level and sub-PFT level. Please define more clearly in section 2.2.1.

Answer 7: We revised this sentence in section 2.1 to “Other processes in the model such as carbon and nitrogen allocation for growth of new tissues respond to this phenology scheme at both PFT level and phytomer level.” (Lines 165-167). Another sentence in the preceding paragraph “The modified phenology subroutine controls the life cycle of each phytomer (sub-PFT level) as well as the planting, stem and root turnover, vegetative maturity (start of fruiting) and final rotation (replanting) of the whole plant (PFT level)” indicates that sub-PFT level refers to phytomers and PFT-level refers to the whole plant (Lines 153-156). We also clarified the concept of sub-PFT in the beginning of section 2: “Each phytomer can be considered a sub-PFT component that has its own prognostic leaf growth and fruit yield capacity...” (Lines 128-129). Details on the two levels of phenology are in the Supplementary materials.

Comment 8: P26 L4-5 It is very hard to see “LAI development also matches well with field measurements” in the Figure 4. Please more explanation for the Figure 4, that is more reader friendly.

Answer 8: We revised the caption of Figure 4 (now Fig. 5) and explained in the Results section 4.1 on the comparison of phytomer LAI with 3 leaf samples from the field (Lines 405-409). The LAI of an individual phytomer does not match perfectly with each leaf sample but they are comparable. It needs to be noted that a phytomer in the model is only meant to represent the average condition of an age-cohort of actual oil palm phytomers across the whole plantation landscape. We added this statement in the Introduction (Lines 105-107).

Comment 9: P27 L1 How did you determine “60-day” for the cumulative periods. 30-day is not enough?

Answer 9: 60-day corresponds to the main period of fruit-filling and oil synthesis for a fruit bunch on a phytomer (added in Lines 432-433). Therefore, we assume the precipitation of a 60-day period before each fruit harvest has most direct influence on yield.

Comment 10: P28 L15 Average LAI of what?

Answer 10: The average LAI of 8 oil palm sites (4 H plots and 4 B plots). We revised this sentence to “The average LAI of the eight sites from the model is comparable with field measurement in 2014 (MPE = 13%)” (Lines 470-471). The validation section has been largely updated with the new Figures 9 and 10. New interpretations on LAI validation are added in Lines 462-469.

Comment 11: Some discussions are included in the results section (ex P29 L1-3). You should remove them carefully.

Answer 11: We removed this and other discussions from the results section. New descriptions on yield validation and site-to-site variability are added (Lines 474-480). Redundancy is largely reduced throughout the text.

Comment 12: P29 L8 What is the meaning of the functionality here? Also, again, discussion concerning with processes in oil palm plantation should be removed from the MS, they must be done in intensive field measurement based studies, not modeling study. I rather want to see application of the model developed in this study, how the model contributes to understand impacts of oil palm expansions.

Answer 12: “functionality” refers to the capability or utility of the CLM-Palm model for simulating oil palm’s phenology, allocation and yield. We changed this word to “utility”. We follow the recommendation to remove the original discussion sections 5.2 and 5.3 concerning hypotheses of oil palm processes. The whole discussion section is largely revised. We now focus on discussing the phytomer phenology and allocation, and the ability and limitation of CLM-Palm for simulating year-to-year variability and site-to-site variation in LAI, yield and NPP based on improved results of Fig. 9 and 10 with different treatment of fertilization.

As answered in the beginning, this paper is focused on model development of CLM-Palm. Phenology and allocation are the base functions for oil palm growth and yield which are important for future large-scale simulations of energy and material cycling across Indonesia and even other regions. Ideas of application are indicated in the discussion. In a following study, a fuller picture of the carbon, water and energy fluxes over the oil palm landscape are being evaluated with Eddy Covariance flux observation data in Sumatra. The CLM-palm model in the CESM/CLM framework also allows coupling with climatic models so that the feedbacks of oil palm expansion to climate can be simulated. The impacts of land cover change driven by oil palm expansion are being examined for Sumatra and Kalimantan over the past two decades in another following study.

Comment 13: P34 Please include limitation of the model in the summary.

Answer 13: The limitation of the model is added in Conclusions: “On the other hand, simulating small-scale site-to-site variation (50m × 50m sites) requires detailed input data on site conditions (e.g. microclimate) and plantation managements that are often not available thus limiting the applicability of the model at small scale. Nevertheless, the CLM-Palm model sufficiently represents the significant region-wide variability in oil palm NPP and yield driven by nutrient input and plantation age in Jambi, Sumatra.” (Lines 577-580)

## Response to Referee #2:

We acknowledge that the current MS is too long and includes lots of redundancy. We try to address the three major concerns of referee #2:

First, in order to reduce the size of manuscript we follow the referee's recommendation to shorten the introduction and model description. The detailed phenology description is now moved to Supplementary materials and the appendix on allocation functions is merged back to main text. The discussion sections are condensed to one section. We now add the model name "CLM-Palm" in both the title and text in order to clarify the concepts of PFT, sub-canopy structure and the phenology and allocation sub-routines of the new palm model. Most of the manuscript is largely rewritten and reorganized in order to improve the coherency and clarity of model description, results and discussion. Now the text is reduced by 30% from 14,000 to 10,000 words.

Second, LAI and yield are indeed the output of CLM. We concentrated the validation with them because the phenology and allocation subroutines we develop for CLM-Palm are the base functions for simulating palm growth and yield which in turn are key mechanisms determining carbon, water and energy fluxes. Our CLM-Palm model combines the functions of an agricultural model, that is, growth and yield prediction, and a land surface model, i.e. energy, water and material cycles between land and atmosphere. We now add the validation with field measured NPP as well (see new Fig. 10), so as to show the ability of CLM-Palm for simulating carbon budget. Due to limited space, more comparisons with eddy covariance measurements of carbon, water and energy fluxes are introduced in following studies.

Third and most important, in this revision we try to address the referee2's concerns on the site-to-site variation by presenting new results of the validation simulations at the 8 independent plots. We now treat the validation plots in Harapan and Bukit regions differently in respect of N fertilization. In the last version all the 8 plots were simulated with the same fertilization scheme as the industrial plantation PTPN-VI but actually the smallholder plots used much less fertilizer and Bukit plots were not fertilized in 2013 and 2014. Details on fertilization is added ([Lines 297-306](#)). New simulation results with two levels of fertilization (regular vs. reduced) significantly improve the modelled site-to-site variability in LAI, yield and NPP (see new Fig. 9 and 10), which matches closely with field data ([Lines 462-484](#)). This revision shows that in order to simulate small-scale variation, input data e.g. microclimate and site management at the same scale would be needed for each individual site which is often not available. Our two-category inputs, including the contrasting treatment of fertilization for the two regions already demonstrate the ability of CLM-Palm to sufficiently represent the region-wide variability in oil palm NPP and yield driven by nutrient input and plantation age in Jambi, Sumatra (see [Lines 532-538](#)).

Nevertheless, we pointed out the possible reasons behind the remaining small discrepancy at few sites (HO1 and BO2) in the discussion and leave space for future improvement (see [Lines 469, 480-484 in results, and Lines 539-551 in discussion](#)). The difficulty to capture the small-scale site-to-site variation is tolerable with a land surface modeling approach, because our palm model developed within CLM is aimed to be run for large areas. There are similar studies using CLM to simulate the LAI and yield of annual crops. For example, Drewniak et

al. 2013 (doi:10.5194/gmd-6-495-2013) did not examine site-to-site variation of LAI and yield and validated LAI only with an individual site for each crop. They did not show direct comparison of simulated yield with observation data. Another recent study by Bilonis et al. 2015 (doi:10.5194/gmd-8-1071-2015) validated the CLM-crop model at two AmeriFlux sites but they also indicated limited transferability of the calibrated parameters across sites.

Towards the general mission of a land surface model, our study demonstrates the ability of the new CLM-Palm model to adequately simulate the average LAI, yield and NPP across multiple sites as well as their inter-annual variability driven by age and precipitation and region-wide site-to-site variability driven by plantation age and N availability in the Jambi, Sumatra. This will allow simulating land use change effects driven by oil palm expansion provided land cover data.

We believe our CLM-Palm model development and validations with multiple oil palm sites are meaningful and provide a basis for future large-scale simulations.

(The line numbers all refer to the revised clean-version manuscript.)

#### **Answers to specific comments:**

Comment 1: P4547L20-21: This is very subjective. To me, it should be something like 0% to call it perfectly.

Answer 1: We rephrased “perfectly” to “notably well” (see Lines 35-36).

Comment 2: P4549L1-2: and at fine time steps (e.g. half-hourly). A ref. is needed.

Answer 2: We revised this sentence to “Although a series of agricultural models exist for simulating the growth and yield of oil palm such as OPSIM (van Kraalingen et al., 1989), ECOPALM (Combres et al., 2013), APSIM-Oil Palm (Huth et al., 2014), PALMSIM (Hoffmann et al., 2014), these models did not aim yet at the full picture of carbon, water and energy exchanges between land and atmosphere and remain to be coupled with climate models.” (Lines 66-70). The references are already given for each agricultural model.

Comment 3: P4550L19-20: even for oil-palm-like plantations (e.g. coconut, date palm etc.). If you didn't validate it, you should not state this.

Answer 3: We deleted this sentence. However, our CLM-Palm model and its sub-canopy structure and phenology and allocation functions are developed with generic interest for other

palm crops (e.g. coconut palm) because these palms share very similar canopy structure and phenology and allocation patterns. This is consistent with the basic concept of plant functional type (PFT) used in land surface modelling, which is defined as a group of species sharing the key ecological functions (e.g. resource allocation) and physical and phenological characteristics. Oil palm and other palms can be well defined as one PFT and fit into our CLM-palm model. We now formally name the new model as CLM-Palm and its application for other palm species would only require a recalibration of the input parameters listed in Tables A1-A3. We add a revised sentence in the abstract: “CLM-Palm is tested here on oil palm only but is meant of generic interest for other palm crops (e.g. coconut)” (Lines 22-23).

Comment 4: P4551L20 (and other places): Don’t use “incl.”. This is not conventional.

Answer 4: We removed all the unconventional abbreviations.

Comment 5: P4558L17: What is mxlivenp? It is explained in Table 1 but not the main text.

Answer 5: The sentence is slightly revised to “Pruning is conducted at one time step if the number of expanded phytomers (including senescent ones) exceeds the maximum number allowed on a palm (mxlivenp).” Here “mxlivenp” refers to the maximum number of expanded phytomers allowed on a palm, which is pretty much self-explaining in the parentheses. This sentence together with detailed phenology description is now moved to Supplementary materials.

Comment 6: P4559L22: C:N ratios? The numbers are way too small in Table 2.

Answer 6: The C:N ratios were in Table B1, not in Table 2. Table B1 is now renamed Table A3 in the Appendix.

Comment 7: P4561L20: It’s unclear how you derive NPP<sub>mon</sub> since it extremely challenging to estimate monthly tree NPP?

Answer 7: We revised the sentence to “where NPP<sub>mon</sub> is the monthly sum of NPP from the previous month calculated with a run-time accumulator in the model.” (see Lines 209-210). NPP<sub>mon</sub> refers to modelled value, not that measured in the field. CLM calculates NPP (gC/m<sup>2</sup>/s) at every half-hour time step. We coded a run-time accumulator in the model to get monthly sum of NPP (gC/m<sup>2</sup>/mon) from the per second NPP flux.



We now also add a validation with field measured NPP which is estimated through measurements of stem, root, leaf, and fruit growth in eight mature oil palm sites (see [Lines 293-296](#) and cited paper).

Comment 8: P4564L23: What are the sizes of the sites?

Answer 8: The PTPN-VI site is 2186 ha. Pompa Air is 5.7 ha. Other 8 sites are 50m × 50m each (added in the text, [Lines 274, 277, 286](#)).

Comment 9: Figure 8b: A simple scatterplot field measures vs. simulated LAI would work.

Answer 9: We use the barplot because it can clearly represent the age-related trend in LAI and nutrient-driven variation across sites (now Figure 9b). It allows comparing point simulations with multiple specific site observations with contrasting conditions and age classes. We add two levels of fertilization treatments for H and B plots, and now the interpretation of this figure is largely updated (please see [Lines 462-471](#)). Furthermore, field measured LAI also has very large variation because we did not directly measure LAI at the plot level but only sampled leaf area and dry weight of individual phytomers and scaled the values up ([Lines 471-473](#)). With this data, it is hard to show the relationship between field measurements and simulated LAI by a scatterplot. The barplot can include error bars of measured LAI and also exhibits remaining discrepancy from individual sites.

CLM-Palm as a land surface model is mainly aimed to simulate the average condition of LAI across sites in the regional scale, which is demonstrated by Fig. 9. The remaining small-scale site-to-site variation is explained in discussion ([Lines 539-549](#)).

**List of major changes in the following track-change manuscript:**

1. Title and abstract are updated to include the model name CLM-Palm.
2. Introduction is condensed and reorganized.
3. Unnecessary information in Section 2 is removed. Section 2.1 is condensed to only include a general description of phenology. Detailed phenology description is now moved to Supplementary materials.
4. The Appendix on allocation functions is merged back to main text in Section 2.2.1.
5. New information on NPP measurement and different fertilization treatments in H and B plots is added in Section 3.1.
6. Figures 9 and 10 on LAI, yield and NPP validation are largely updated because of two levels of fertilization. Other figures are slightly updated because of recalibration of model with field measured leaf C:N ratio and slightly updated harvest data.
7. The subsections 5.2 and 5.3 are largely removed and the discussions are condensed into one section.
8. New results and discussions based on Fig. 9 and 10 are added in Section 4.3 and 5.
9. The tables are all moved to Appendix (Table A1-A3).
10. Reference list is updated.

A sub-canopy structure for simulating oil palm in the Community Land Model ([CLM-Palm](#)):  
phenology, allocation and yield

Yuanchao Fan<sup>1,2,\*</sup>, Olivier Roupsard<sup>3,4</sup>, Martial Bernoux<sup>5</sup>, Gueric Le Maire<sup>3</sup>, Oleg Panferov<sup>6</sup>,  
Martyna M. Kotowska<sup>7</sup>, Alexander Knohl<sup>1</sup>

<sup>1</sup> University of Göttingen, Department of Bioclimatology, Büsgenweg 2, 37077 Göttingen,  
Germany

<sup>2</sup> AgroParisTech, SIBAGHE ([Systèmes intégrés en Biologie, Agronomie, Géosciences,  
Hydrosciences et Environnement](#)) ~~Doctoral School~~, 34093 Montpellier, France

<sup>3</sup> CIRAD, UMR Eco&Sols (Ecologie Fonctionnelle & Biogéochimie des Sols et des Agro-  
écosystèmes), 34060 Montpellier, France

<sup>4</sup> CATIE (Tropical Agricultural Centre for Research and Higher Education), 7170 Turrialba,  
Costa Rica

<sup>5</sup> IRD, UMR Eco&Sols, 34060 Montpellier, France

<sup>6</sup> University of Applied Sciences Bingen, 55411 Bingen am Rhein, Germany

<sup>7</sup> University of Göttingen, Department of Plant Ecology and Ecosystems Research, Untere  
Karspüle 2, 37073 Göttingen, Germany

\*Correspondence author. E-mail: yfan1@uni-goettingen.de

**Abstract:** ~~Land surface modelling has been widely used to characterize the two-way interactions between climate and human activities in terrestrial ecosystems such as deforestation, agricultural expansion, and urbanization. Towards an effort~~ In order to quantify the effects of forests to oil palm conversion occurring in the tropics on land-atmosphere carbon, water and energy fluxes, we ~~develop~~introduce a new perennial crop sub-model CLM-Palm for simulating a palm plant functional type (PFT) ~~for oil palm. Due to the modular and sequential nature of oil palm growth (around 40 stacked phytomers) and yield (fruit bunches axillated on each phytomer), we developed a specific sub-canopy structure for simulating palm's growth and yield~~ within the framework of the Community Land Model (CLM4.5). CLM-Palm is tested here on oil palm only but is meant of generic interest for other palm crops (e.g. coconut). The oil palm has monopodial morphology and sequential phenology of around 40 stacked phytomers, each carrying a large leaf and a fruit bunch, forming a multilayer canopy. A sub-canopy phenological and physiological parameterization is thus introduced, so that ~~In this structure~~ each phytomer has its own prognostic leaf growth and fruit yield capacity ~~like a PFT~~ but with shared stem and root components ~~among all phytomers~~. Phenology and carbon and nitrogen allocation operate on the different phytomers in parallel but at unsynchronized steps, separated by a thermal period so that multiple fruit yields per annum are enabled in terms of carbon and nitrogen outputs. An important phenological phase is identified for the palm PFT - the storage growth period of bud and “spear” leaves which are photosynthetically inactive before expansion. Agricultural practices such as transplanting, fertilization, and leaf pruning are represented. Parameters introduced for the new PFT oil palm were calibrated and validated with field measurements of leaf area index (LAI), ~~and~~ and net primary production (NPP) from Sumatra, Indonesia. In calibration with a mature oil palm plantation, the cumulative yields from 2005 to 2014 matched notably well~~perfectly~~ between simulation and observation (mean percentage error = 43%). Simulated inter-annual dynamics of PFT-level and phytomer-level LAI were both within the range of field measurements. Validation from eight independent oil palm sites shows the ability of the model to adequately predict the average leaf growth and fruit yield across sites and sufficiently represent the significant nitrogen and age related site-to-site

48 | variability in NPP and yield. Results~~but~~ also indicates that seasonal dynamics of yield and  
49 | remaining small-scale site-to-site variability of ~~yield-NPP~~ are driven by processes not yet  
50 | implemented in the model or reflected in the input data. The new sub-canopy structure and  
51 | phenology and allocation functions now allow exploring the effects of tropical land use  
52 | change, from natural ecosystems to oil palm plantations, on carbon, water and energy cycles  
53 | and regional climate.

## 1. Introduction

Land-use changes in South-East Asia's ~~tropical regions~~ have been accelerated by economy-driven expansion of oil palm (*Elaeis guineensis*) ~~plantations-agriculture~~ since the 1990s (Miettinen et al., 2011). Oil palm is currently one of the most rapidly expanding and high-yielding crops in the world (Carrasco et al., 2014) and Indonesia as the largest global palm-oil producer is planning to double its oil-palm area from 9.7 million ha in 2009 to 18 million ha by 2020 (Koh and Ghazoul, 2010). Since oil palms favor a tropical-humid climate with consistently high temperatures and humidity, the plantation expansion has converted large areas of rainforest in Indonesia in the past two decades ~~replacing including those mainly intact forests (47%), logged forests (22%), and agroforests (21%) and also happening~~ on carbon-rich peat soils ~~(-10%)~~ (Carlson et al., 2012; Gunarso et al. 2013).

~~Tropical deforestation caused by the expansion of oil palm plantations has significant implications on above- and below-ground carbon stocks (Kotowska et al., 2015).~~ Undisturbed forests have ~~a significantly higher~~ long-lasting capacity to store carbon ~~than in comparison to~~ disturbed or managed vegetation (Luyssaert et al., 2008). Tropical forest to oil palm conversion has significant implications on above- and belowground carbon stocks (Kotowska et al., 2015a). However, the exact quantification of long-term and large-scale forest – oil palm replacement effects is difficult as the greenhouse gas balance of oil palms is still uncertain due to incomplete monitoring of the dynamics of oil palm plantations (including young development stage), and lack of understanding of the carbon, nitrogen, water and energy exchange between oil palms, soil and the atmosphere at ecosystem scale. Besides that, the assessment of these processes in agricultural ecosystems is complicated by human activities e.g. crop management, including planting and pruning, irrigation and fertilization, litter and residues management, and yield outputs. One of the suitable tools for evaluating the feedback of oil palm expansion is ecosystem modelling. The greenhouse gas balance of oil palms is still uncertain due to incomplete monitoring of the development of young oil palm plantations,

and lack of understanding of the carbon and nitrogen exchange between oil palm, soil and the atmosphere at ecosystem scale. The dynamics of greenhouse gases such as CO<sub>2</sub>, N<sub>2</sub>O and CH<sub>4</sub> in agricultural ecosystems also depends on crop management, such as planting and pruning, irrigation and fertilization, management of litter and residues (burning, windrowing), processing and exports (e.g. yield and litter outputs). Although a series of agricultural models exist for simulating the growth and yield of oil palm such as OPSIM (van Kraalingen et al., 1989), ECOPALM (Combres et al., 2013), APSIM-Oil Palm (Huth et al., 2014), PALMSIM (Hoffmann et al., 2014), ~~they are not meant for studying these models did not aim yet at~~ the full picture of carbon, water and energy exchanges between land and atmosphere and remain to be coupled with climate models at large ecosystem scales and at fine time steps (e.g. half-hourly). Given the current and potential large-scale deforestation driven by the expansion of oil palm plantations, the ecosystem services such as yield, carbon sequestration, microclimate, energy and water balance of this new managed oil palm landscape have to be evaluated in order to quantify with precision the overall impact of land-use change on environment including regional and global climate.

Land surface modelling has been widely used to characterize the two-way interactions between climate and human activities in terrestrial ecosystems such as deforestation, agricultural expansion, and urbanization (Jin and Miller, 2011; Oleson et al., 2004). A variety of land models have been adapted to simulate land surface-atmosphere energy and matter exchanges for major crops such as the Community Land Model (CLM, LPJmL, JULES, ORCHIDEE models, etc. CLM is the land component of the Community Earth System Model (CESM). It simulates three major components of terrestrial ecosystem processes: surface energy fluxes, hydrology, and biogeochemical cycles (Oleson et al., 2013). The model-CLM represents the land surface as a hierarchy of sub-grid types: glacier, lake, urban, crop, and vegetated land. Ccrop and ~~(naturally)~~ vegetated land units ~~are further represented~~ as patches of plant functional types (PFTs) defined by their key ecological functions (Bonan et al., 2002). However, most of the crops being simulated are annual crops such as wheat, corn, soybean,

107 | ~~rice~~, etc. Their phenological cycles are usually represented as ~~multiple-three~~ stages of  
108 | development from planting to leaf emergence, to fruit-fill and to harvest, all within a year.  
109 | Attempts were also made to evaluate the climate effects of perennial crops, e.g. by extending  
110 | the growing season of annuals (Georgescu et al., 2011). However the perennial crops such as  
111 | oil palm, cacao, coffee, rubber, coconut, and other fruiting trees and their long-term  
112 | biophysical processes are not represented in the above land models yet, despite the worldwide  
113 | growing demand (FAO, 2013). ~~Furthermore, most crops are harvested once per year and the~~  
114 | ~~impact of yield output on carbon flux and carbon stock should be investigated at the inter-~~  
115 | ~~annual time scale.~~

116 | Oil palm is a perennial evergreen crop ~~which can be described by following~~ the Corner's  
117 | architectural model (Hall et al., 1978), ~~each phytomer carrying a large leaf (or frond)~~  
118 | ~~axillating a fruit bunch~~. A number of phytomers, ~~each carrying a large leaf and axillating a~~  
119 | ~~fruit bunch~~, emerge successively (nearly two per month) from a single meristem (the bud) at  
120 | the top of a solitary stem. ~~These phytomers develop in series throughout their life cycles,~~  
121 | ~~being on top of the crown at emergence, then, They form a multilayer canopy with old leaves~~  
122 | progressively being covered by new ~~phytomers~~, until ~~being pruned at~~ senescence. Each  
123 | ~~phytomer~~ has its own phenological stage and yield, according to respective position in the  
124 | crown. ~~The oil palm is productive for more than 25 years, including a juvenile stage of around~~  
125 | ~~2 years. Carbon (C) and nitrogen (N) allocation also has to be determined for each phytomer~~  
126 | ~~specifically according to its phenology. The corresponding gross primary production (GPP)~~  
127 | ~~by leaves and carbon output by fruit harvests both exhibit seasonal dynamics in response to~~  
128 | ~~environmental drivers and agricultural managements.~~ In order to capture the inter- and intra-  
129 | annual dynamics of ~~growth and yield and land-atmosphere energy, water and carbon fluxes~~  
130 | ~~land-atmosphere fluxes~~ in the oil palm system, a new structure and dimension detailing the  
131 | ~~phytomer-level sub-canopy phenological~~phenology, ~~carbon (C)~~ and ~~nitrogen (N)~~ allocation  
132 | and agricultural management ~~processes~~ has to be added to the current integrated plant-level  
133 | ~~biogeochemical-physiological~~ parameterizations in the land models. This specific refinement

needs to remain compliant with the current model structure though, and be simple to parameterize.

In this study context, we develop a new CLM-Palm sub-model sub-canopy phytomer-based structure for simulating an “oil palm plantation” land use the growth, yield, and energy and material cycling of oil palm within the framework of the Community Land Model (CLM4.5). ~~The new phytomer-based structure is designed for a special oil palm PFT, or even for oil-palm-like plantations (e.g. coconut, date palm etc.).~~ It introduces a sub-canopy phenological and physiological parameterization, so that multiple leaf and fruit components operate in parallel but at delayed steps, ~~separated by a thermal period. More specifically, at the PFT level vegetative growth is represented by leaf development of different age cohorts (40 ranks) of phytomers as well as the development of shared stem and root. Reproductive growth of the PFT consists of simultaneous fruit filling at different age cohorts of bunches, and yield includes multiple harvests per year of the mature bunches at the lower end of the canopy. The phenology is driven by thermal time and available C and N are allocated accordingly to the vegetative and reproductive components for the whole plant and then partitioned between phytomers. A phytomer in the model is meant to represent the average condition of an age-cohort of actual oil palm phytomers across the whole plantation landscape. The overall gross primary production (GPP) by leaves and carbon output by fruit harvests rely on the development trends of individual phytomers.~~ The functions implemented for oil palm combine the characteristics of both trees and crops, such as the woody-like stem growth and turnover but the crop-like vegetative and reproductive allocations which enable fruit C and N output. Agricultural practices such as transplanting, fertilization, and leaf pruning are also represented.

~~Overall, this new parameterization on oil palm aims to allow future investigation of the effects of forest (forest PFTs already available in CLM) to oil palm conversion on carbon, water and energy fluxes between land and atmosphere across regional to global scales.~~



The main objectives of this paper are to: i) describe the development of CLM-Palm ~~the new sub-canopy structure for oil palm in the CLM~~ including its phenology, carbon and nitrogen allocation, and yield output; ii) optimize model parameters using field-measured leaf area index (LAI) and observed long-term monthly yield data from a mature oil palm plantation in Sumatra, Indonesia; and iii) validate the model against independent LAI, yield and net primary production (NPP) data from eight oil palm plantations of different age in Sumatra, Indonesia.

## 2. Model development

~~The crop model component of CLM4.5 implements the interactive crop management parameterizations from the land surface model AgroIBIS (Kucharik and Brye, 2003; Levis et al., 2012; Drewniak et al., 2013). It has explicit representations of crop type, planting, harvesting, fertilization, and irrigation. The managed crop types currently simulated and validated in CLM4.5 include corn, soybean, and temperate cereals (incl. spring wheat, barley, and rye). All of them are annual crops and follow the same 3 phase phenological cycle: from planting to leaf emergence, to beginning of fruit fill, and to harvest. The initiation and ending of each phase are determined by an accumulation of heat measured with growing degree days (GDD; White et al., 1997). Carbon and nitrogen allocation for growth of new tissues is determined for leaf, stem, root and grain components and changes dynamically corresponding to the phenological phases. The plant canopy is approximated as a big leaf and its growth allocation starts from leaf emergence and declines continuously until zero when grain fill begins. Since grain fill, the LAI declines drastically because of background litter fall controlled by leaf longevity. Furthermore, the entire yield represented by grain C and N is currently routed into the litter pool in CLM4.5.~~

~~For the adequate description of oil palm functioning, these simplifications are not sufficient and the structure of the CLM crop model should be adapted. First, oil palm is a perennial evergreen crop and thus the annual phenological cycle has to be extended to perennial.~~

~~Second, allocation functions have to be modified accordingly for an evergreen pattern. Third and most important, a multiple growth and yield scheme that can respond to seasonal climatic dynamics has to be coined for oil palm's continuous fruit filling and harvests throughout a year. Lastly, it would be more logical to output the harvested fruit C into a separate export C pool instead of routing it to litter. This is necessary to enhance the decomposition computation and allows the validation against observed yield data and soil carbon data.~~

For adequate description of oil palm functioning, we adapt the CLM crop phenology, allocation and vegetation structure subroutines to the monopodial morphology and sequential phenology of oil palm so that A sub-canopy structure can meet most of the above needs by ~~dividing the canopy into multiple layers or multiple “big leaves”, each phytomer having its own phenology, evolves independently in~~ growth and yield (Fig. 1a). ~~An oil palm produces successively 20-30 phytomers every year according~~Their phenology sequence is determined by the ~~to~~ phyllochron (the period in heat unit between initiations of two subsequent phytomers) (Table A1~~Fig. 1b~~). ~~Each phytomer carries a large leaf (frond) and an axillated inflorescence bunch.~~ A maximum of 40 phytomers with expanded leaves, each growing up to 7-m long, are usually maintained in plantations by pruning management, ~~eliminating senescent leaves at the bottom of the crown.~~ There are also around 60 initiated phytomers developing slowly inside the bud, ~~all being heterotrophic.~~ The eldest-largest ones, already emerged at the top of the crown ~~and but~~ unexpanded yet, are named “spear” leaves (Fig. 1a). Each phytomer can be considered a sub-PFT component that has its own prognostic leaf growth and fruit yield capacity ~~like a PFT~~ but having 1) the stem and root components that are shared by all phytomers, 2) the soil water content, nitrogen resources, and resulting photosynthetic assimilates that are also shared and partitioned among all phytomers, and 3) a vertical structure of the foliage, with the youngest at the top and the oldest at the bottom of the canopy. Within a phytomer the fruit and leaf components do not compete for growth allocation because leaf growth usually finishes well before fruit-fill starts. However one

phytomer could impact the other ones through competition for assimilates, which is controlled by the C and N allocation module according to their respective phenological stages.

~~The phytomer configuration is similar to the one already implemented in other oil palm growth and yield models such as the APSIM Oil Palm model (Huth et al., 2014) or the ECOPALM yield prediction model (Combres et al., 2013). However, the implementation of this sub-canopy structure within the CLM modeling framework is the first attempt among land surface models. It incorporates the ability of yield prediction, like an agricultural model, beside that it allows the modeling of both biophysical and biogeochemical processes as a land model should do, e.g. what is the whole fate of carbon in plant, soil and atmosphere if land surface composition changes from a natural system to the managed oil palm system?~~

~~In this model description,~~Here we ~~focus on~~describe only the new phenology, allocation and agricultural management functions developed specifically for the oil palm—~~PFT~~. Photosynthesis, respiration, water and nitrogen cycles and other biophysical processes ~~are the important functions~~ already implemented in CLM4.5 (Oleson et al. (2013) and ~~they~~ are not modified (except N retranslocation scheme) for the current study. ~~Details about these functions can be found in Oleson et al. (2013).~~ The following diagram shows the major model developments in this paper and their coupling with existing modules within the CLM4.5 framework (Fig. 2).

## 2.1. Phenology

~~In CLM, three types of phenologies (evergreen, seasonal deciduous and stress deciduous) are available for natural PFTs. These phenology algorithms provide prognostic controls on the seasonal timing of new leaf growth (onset) as well as leaf litter fall (offset) and root and stem turnovers. The crop PFTs have a separate phenology, which has additional steps to control reproductive growth and harvest. For annual crops, it is sufficient to consider the 3-phase phenological cycle for the plant whole life. Leaves are assumed to grow until grain fill and~~

~~harvest implies removal of the reproductive part as well as of all the vegetative components  
incl. leaf, stem and root.~~

~~The oil palm, as a perennial evergreen crop, is fundamentally distinct from the natural  
vegetation and other types of crops. It has to sustain a high level of LAI while producing  
fruits continuously (nearly two fruit bunches per month) for many years, including a juvenile  
stage. In order to simulate such phenology, the vegetative growth must be partially decoupled  
from the reproductive growth. For example, leaf growth and maturity could be finished well  
before fruit fill and leaf senescence could happen after a harvest event. Moreover, each  
phytomer has its own phenology that controls its leaf and fruit development (Fig. 1).~~

~~We designed six post-planting phases for the phytomer phenology: 1) from leaf initiation to  
leaf expansion; 2) from leaf expansion to leaf maturity; 3) from leaf maturity to fruit fill; 4)  
from fruit fill to harvest; 5) from harvest to leaf senescence; and 6) from leaf senescence to  
pruning (Fig. 1b). The modified phenology module controls the life cycle of each phytomer as  
well as the stem and root turnover for the whole plant. Different~~

Establishment of the oil palm plantation is implemented with two options: seed sowing or  
transplanting of seedlings. In this study, the transplanting option is used. We design 7 post-  
planting phenological steps for the development of each phytomer: 1) leaf initiation; 2) start  
of leaf expansion; 3) leaf maturity; 4) start of fruit-fill; 5) fruit maturity and harvest; 6) start of  
leaf senescence; and 7) end of leaf senescence and pruning (Fig. 1b). The first two steps  
differentiate pre-expansion (heterotrophic) and post-expansion (autotrophic) leaf growth  
phases. The other steps control leaf and fruit developments independently so that leaf growth  
and maturity could be finished well before fruit-fill and leaf senescence could happen after  
fruit harvest according to field observations. The modified phenology subroutine controls the  
life cycle of each phytomer (sub-PFT level) as well as the planting, stem and root turnover,  
vegetative maturity (start of fruiting) and final rotation (replanting) of the whole plant (PFT  
level). Detailed description of oil palm phenology and nitrogen retranslocation during

senescence is in the Supplementary materials. The main phenological parameters are in Table A1.

All phytomers are assumed to follow the same phenological steps, and where the same thermal length for each phase. Air temperature is the key variable or “clock” for the phytomer phenology as is measured by growing degree-days (GDD; White et al., 1997) GDD. For tropical crops such as oil palm, a new GDD variable with 15 °C base temperature and 25 degree-days daily maximum (Corley and Tinker, 2003; Goh, 2000; Hormaza et al., 2012) is accumulated since planting (abbr. GDD<sub>15</sub>). The six phenological phases are signaled by respective GDD requirements, except that pruning is controlled by the maximum number of live-expanded phytomers according to plantation management (Table A1). Other processes in the model such as carbon and nitrogen allocation for growth of new tissues respond to this phenology scheme for growth of new tissues at both the PFT level and sub-PFT phytomer level (section 2.2).

(Sections 2.1.1 to 2.1.7 are all moved to Supplementary materials)

#### 2.1.1. Planting and leaf initiation

Planting is implemented in the similar way as in the CLM4.5 crop phenology except that GDD<sub>15</sub> is tracked since planting and an option of transplanting is enabled. An initial phytomer emergence threshold ( $GDD_{init}$ ) is prescribed for attaining the first leaf initiation after planting (Table 1). When  $GDD_{init}$  is zero, it implies transplanting from nursery instead of seed sowing in the field. Oil palm seedlings usually grow in nursery for 1-2 year before being transplanted into the field. Therefore, in this study  $GDD_{init}$  is set to zero and the first new phytomer is assumed to initiate immediately after transplanting in the field. An initial total LAI of 0.15 is assigned to the existing expanded phytomers, whose leaf sizes are restricted to be within 10% of  $PLAI_{max}$  (Table 2).

The oil palm phytomers initiate as leaf primordia in the apical bud and then appear as leaves on the stem successively according to relatively stable intervening periods, termed plastochron (the duration in terms of heat unit (GDD) between successive leaf initiation events) and phyllochron (the rate of leaf emergence from the apical bud). Here for simplicity, the phyllochron is assumed equal to the plastochron. As the apical buds in palms usually do not start to accumulate dry mass immediately after physiological initiation but wait until several phyllochrons before expansion (Navarro et al., 2008), we define leaf initiation as the start of active accumulation of leaf C in this model, so that the phenological steps and C and N allocation process can be at the same pace.

A parameter *phyllochron* is prescribed with an initial value of 130 degree days at planting with reference to  $GDD_{15}$  and it increases linearly to 1.5 times at 10-year old (Huth et al., 2014; von Uexküll et al., 2003). Given  $GDD_{init}$  and *phyllochron*, a heat unit index  $H_p^{init}$  for triggering leaf initiation can be calculated for each new phytomer when a preceding phytomer initiates:

$$\frac{H_{p+1}^{init} - GDD_{init}}{H_p^{init} - H_p^{init} + \text{phyllochron}} \quad \text{Eq. 1}$$

where subscripts  $p$  and  $p+1$  refer to successive phytomers and  $1$  refers to the first new phytomer initiated after planting.

As the GDD accumulates since planting, new phytomers will be turned on in sequence when  $GDD_{15} > H_p^{init}$ , and will enter the 6-phase life cycle one by one. The timing of later phenological steps for each new phytomer is determined at the time of initiation by adding the length of a corresponding phase period (Table 1). Each newly initiated phytomer is assigned a negative rank of  $-N$  and remains packed in the bud until the next phase of leaf expansion is triggered. The oldest unexpanded phytomer (spear leaf), right before expansion, has a rank of

~~1. The GDD period between leaf initiation and expansion is used to calculate the number of bud phytomers that have already initiated before transplanting, i.e.  $N = \frac{GDD_{exp}}{phyllchron}$ .~~

### ~~2.1.2. Leaf expansion~~

~~During the phase from initiation to leaf expansion, leaf C already starts to build up in the bud or spear leaf but it remains photosynthetically inactive. The thermal threshold for leaf expansion is calculated by  $H_p^{exp} = H_p^{init} + GDD_{exp}$ . Only when  $GDD_{15} > H_p^{exp}$  for a phytomer ranked -1, the leaf starts to expand and becomes photosynthetically active. Its rank changes to a positive value of 1, while the ranks of other phytomers all increase by 1 at the same time. The expansion phase lasts for roughly 5-6 phyllochrons until leaf maturity (Legros et al., 2009).~~

~~Hereafter, the pre-expansion and post-expansion growth periods, distinguished by negative and positive ranks, are treated separately so as to differentiate non-photosynthetic and photosynthetic increases in leaf C. The following post-expansion phases and their thresholds are determined with reference to  $H_p^{exp}$ .~~

### ~~2.1.3. Leaf maturity~~

~~Another phenological step is added for the timing of leaf maturing so as to control the period of post-expansion leaf growth for each phytomer. An oil palm leaf usually reaches maturity well before fruit fill starts on the same phytomer. Therefore, we set the parameter  $GDD_{L.mat}$  to be smaller than  $GDD_{F.fill}$  (Table 1) so that post-expansion leaf growth continues for 2-3 months (5-6 phyllochrons) and stops around 6 months before fruit fill. The phenological threshold  $H_p^{L.mat}$  is calculated as  $H_p^{L.mat} = H_p^{exp} + GDD_{L.mat}$ .~~

### ~~2.1.4. Fruit filling~~

Fruit fill starts on a phytomer when  $GDD_{15}$  exceeds a heat unit index  $H_p^{F.fill}$ . This threshold is calculated by  $H_p^{F.fill} = H_p^{exp} + GDD_{F.fill}$ . At this point, the phytomer enters reproductive growth. Growth allocation increases gradually for the fruit component while leaf C and LAI remain constant on the mature phytomer until senescence. Due to the fact that most inflorescences on the initial phytomers within 2 years after planting are male (Corley and Tinker, 2003), another threshold  $GDD_{min}$  is used to control the beginning of first fruiting on the palm. Only when  $GDD_{15} > GDD_{min}$ , the mature phytomers are allowed to start fruit-filling.

#### 2.1.5. Fruit harvest and output

Fruit harvest occurs at one time step when a phytomer reaches fruit maturity, measured by a heat unit index  $H_p^{F.mat} = H_p^{exp} + GDD_{F.mat}$ . Since GDD build-up is weather dependent and phyllochron increases through aging, the harvest interval is not constant. New variables track the flow of fruit C and N harvested from each phytomer to PFT level crop yield output pools. The fruit C and N outputs are isolated and are not involved in any further processes such as respiration and decomposition, although their fate is largely uncertain.

#### 2.1.6. Litter fall

For oil palm, leaf litter fall is performed in two phases: senescence and pruning. Senescence is simulated as a gradual reduction in photosynthetic leaf C and N on the bottom phytomers when  $GDD_{15} > H_p^{L.sen}$ , where  $H_p^{L.sen} = H_p^{exp} + GDD_{L.sen}$ . These phytomers are allowed to stay on the palm until pruning is triggered. Their senescence rates are calculated as the inverse of the remaining time until the end of a phytomer's life cycle ( $GDD_{end}$ ). Leaf C removed during this phase is not put into the litter pool immediately but saved in a temporary pool  $C_{leaf}^{senescent}$  until pruning, while the photosynthetic LAI of senescent phytomers are updated at every time step. The reason to do this is that each oil palm frond is a big leaf



attached tightly to the stem and its leaflets do not fall to the ground during senescence unless the whole frond is pruned. Thus, the dynamics of soil litter pool and decomposition process could be represented better with this function. Nitrogen from senescent phytomers is remobilized to a separate N retranslocation pool that contributes to photosynthetic N demand of other phytomers and avoids supplying excessive amount of N to the litter. The proportion of N remobilized from senescent leaves before pruning is adjusted by the length of senescent period ( $GDD_{end} - GDD_{L, sen}$ ) with a given pruning frequency, and the rest N goes to the litter pool.

Pruning is conducted at one time step if the number of expanded phytomers (incl. senescent ones) exceeds the maximum number allowed (i.e.  $mxlivenp$ ). All senescent phytomers are subject to pruning at the time of harvest and their remaining C and N together with the temporary  $C_{leaf}^{senescent}$  pool are moved to the litter pool immediately. The frequency and intensity of pruning is determined through the combination of  $mxlivenp$ ,  $GDD_{L, sen}$  and  $phyllochron$ . A larger  $mxlivenp$  gives lower pruning frequency and a smaller  $GDD_{L, sen}$  results in more senescent leaves being pruned at one time. Besides, since  $phyllochron$  increases by age, the rate of phytomer emergence decreases and thus pruning frequency also decreases when the plantation becomes older.

#### 2.1.7. Stem, roots and rotation

Unlike other crops, the oil palm stem is represented by two separate pools for live and dead stem tissues (Fig. 1a). Although the stem of oil palm is not truly woody, field observations have found that the stem section below the lowest phytomer only contains less than 6% of live tissues in the core of trunk for transporting assimilates to the roots (van Kraalingen et al., 1989). This is similar to the stem of most woody trees that largely consists of functionally dead lignified xylem. Therefore, conversion from live to dead stem for oil palm follows the CLM stem turnover function for trees, except that the turnover rate is slightly adjusted to be the inverse of leaf longevity (in seconds), such that when a leaf is dead the stem section below

~~it will mostly become dead. Leaf longevity is around 1.6 years measured from leaf expansion to the end of senescence. The oil palm fine root turnover follows the CLM scheme for trees and crops which also uses a turnover rate as the inverse of leaf longevity. When the maximum plantation age (usually 25 years) of oil palm is reached and a new rotation cycle starts, the whole PFT is turned off and all C and N of the leaves, stem and roots go to litter. Existing fruit C and N of mature phytomers go to the fruit output pools. The PFT is then replanted in the next year and enters new phenological cycles.~~

## 2.2. Carbon and Nitrogen allocation

~~In the CLM model plant growth, yield, stem turnover and litter fall are simulated as the expansion and shrinking of C and N pools of the leaf, stem, root and grain/fruit components, and mediated by the developmental stage (phenology), atmospheric forcing, and N supply along with other environmental factors. In CLM, the fate of newly assimilated carbon from photosynthesis is determined by a coupled C and N allocation routine. Potential allocation for new growth of various plant tissues is calculated based on allocation coefficients and their allometric relationship C:N ratios for each tissue type (Table A2). The C:N ratios link C demand and N demand so that a N down-regulation mechanism is enabled for scaling down potential GPP depending on N-availability from soil mineral N or retranslocated N pool.~~

~~Here allocation refers to the partitioning of remaining photosynthetic carbon for the new growth of various tissues, after accounting for their respiration costs and N down-regulation. Photosynthesis calculation is based on the model of Farquhar et al. (1980). Stomatal conductance is linked to net leaf photosynthesis and scaled by the relative humidity and CO<sub>2</sub> concentration at the leaf surface as well as soil water stress (Collatz et al., 1991; Sellers et al., 1996). Only expanded leaves and the remaining photosynthetically active part of senescent leaves are involved in the photosynthesis process. Maintenance respiration is calculated as a function of temperature and the C and N content of each live vegetation component (Ryan, 1991). The major fraction of stem tissue is dead and thus excluded from respiration processes.~~

CLM assumes a common base rate of maintenance respiration per unit N content for all live tissue types. The carbon cost of maintenance respiration at daytime is subtracted from available photosynthetic C pool before its allocation to new growth. Growth respiration cost is set as a constant percentage (25%) of allocated C to new growth (Oleson et al., 2013). The above photosynthesis and respiration mechanisms, already existing in CLM4.5, are well coupled with the new growth allocation mechanism and the sub-canopy structure for oil palm (Fig. 2).

A two-step allocation scheme is designed for the ~~multilayer~~ sub-canopy phytomer structure and according to the new phenology ~~described in section 2.1~~. First, available C (after subtracting respiration costs) is partitioned to the root, stem, overall leaf, and overall fruit pools with respect to their relative demands by dynamic allocation functions according to PFT-level phenology at the PFT level. Available N is allocated accordingly by the C:N ratios. The C:N ratios for different tissues link C demand and N demand so that a N down-regulation mechanism is enabled to rescale GPP and C allocation if N availability from soil mineral N pool and retranslocated N pool does not meet the demand. Then, the actual C and N allocated to the overall leaf or fruit ~~is~~ pools are partitioned between different phytomers at the sub-PFT level (Fig. 2). Details are described below.

#### 2.2.1. PFT level allocation

Corley and Tinker (2003) described an “overflow” model that oil palm produces vegetative dry matter at a relatively constant rate after maturity and only the excess assimilates go to the reproductive pool, which can guide the partitioning of available assimilates between vegetative and reproductive pools. In our module, C and N allocation at the PFT level is treated at two distinct phenological phases. Before fruiting starts (i.e.  $GDD_{15} < GDD_{mtn}$ ) all the allocation goes to the vegetative components. The initial allocation coefficients (Table 2) are used to partition available C and N to the leaf, stem, and root pools (Eqs. A1–3 in Appendix). The root allocation ratio declines linearly throughout life and allocations to leaf

and stem increase slightly. After fruiting begins, the vegetative allocation ratios continue to approach their final values with dynamic functions (Eqs. A4-6 in Appendix). The leaf allocation ratio increases with a convex shape if the parameter  $d_{alloc}^{leaf} < 1$  and a concave shape if  $d_{alloc}^{leaf} > 1$  until it stabilizes at a certain age determined by  $d_{mat}$ . Real-time allocation to stem is partitioned to its live and dead stem tissues by the ratio  $F_{stem}^{live}$ . The live portion is then involved in stem turnover (section 2.1.7).

C and N allocation at the PFT level is treated distinctly before and after oil palm reaches vegetative maturity. At the juvenile stage before fruiting starts (i.e.  $GDD_{15} < GDD_{min}$ ) all the allocation goes to the vegetative components. The following equations are used to calculate the allometric ratios for partitioning available C and N to the leaf, stem, and root pools.

$$A_{root} = a_{root}^i - (a_{root}^i - a_{root}^f) \frac{DPP}{Age_{max}}, \quad (Eq. 1)$$

$$A_{leaf} = f_{leaf}^i \times (1 - A_{root}) \quad (Eq. 2)$$

$$A_{stem} = 1 - A_{root} - A_{leaf} \quad (Eq. 3)$$

where  $\frac{DPP}{Age_{max}} \leq 1$ ,  $DPP$  is the days past planting, and  $Age_{max}$  is the maximum plantation age (~25 years).  $a_{root}^i$  and  $a_{root}^f$  are the initial and final allocation coefficients for roots and  $f_{leaf}^i$  is the initial leaf allocation coefficient before fruiting (Table A2). Root and stem allocation ratios are calculated with Eqs. 1 and 3 for all ages and phenological stages of oil palm.

After fruiting begins, the new non-linear function is used for leaf allocation:

$$A_{leaf} = a_{leaf}^2 - (a_{leaf}^2 - a_{leaf}^f) \left( \frac{DPP - DPP_2}{Age_{max} \times d_{mat} - DPP_2} \right)^{d_{alloc}^{leaf}} \quad (Eq. 4)$$

where  $a_{leaf}^2$  equals the last value of  $A_{leaf}$  calculated right before fruit-fill starts and  $DPP_2$  is the days past planting right before fruit-fill starts.  $d_{mat}$  controls the age when the leaf allocation ratio approaches its final value  $a_{leaf}^f$ , while  $d_{alloc}^{leaf}$  determines the shape of change (convex when  $d_{alloc}^{leaf} < 1$ ; concave when  $d_{alloc}^{leaf} > 1$ ).  $A_{leaf}$  stabilizes at  $a_{leaf}^f$  when  $DPP \geq Age_{max} d_{mat}$ . The equations reflect changed vegetative allocation strategy that reduces stem and root growth rates and shifts resources to leaf for maintaining LAI and increasing photosynthetic productivity when fruiting starts. The three vegetative allocation ratios  $A_{leaf}$ ,  $A_{stem}$  and  $A_{root}$  always sum to 1.

At the ~~reproductive~~ second phase ~~when fruit fill begins~~ a fruit allocation ratio  $A_{fruit}$  is introduced, which is relative to the total vegetative allocation unity. To represent the dynamics of reproductive allocation effort of oil palm during its development, we adapt the stem allocation scheme for woody PFTs in CLM, in which increasing ~~net primary production~~ (NPP) results in increased allocation ratio for the stem wood (Oleson et al., 2013). We use the similar formula for reproductive allocation of oil palm so that it increases with increasing NPP:

$$A_{fruit} = \frac{2}{1 + e^{-b(NPP_{mon} - 100)}} - a \quad (\text{Eq. 25})$$

where  $NPP_{mon}$  is the monthly sum of NPP from the previous month ~~and~~ calculated with a run-time accumulator in the model. The number 100 (gC/m<sup>2</sup>/mon) is the base monthly NPP when the palm starts to yield (Kotowska et al., 2015). Parameters  $a$  and  $b$  adjust the base allocation rate and the slope of curve, respectively (Table A2). This function generates a dynamic curve of ~~coefficient~~  $A_{fruit}$  increasing from the beginning of fruiting to full vegetative maturity, which is used in the allocation allometry to partition assimilates between vegetative and reproductive pools (Fig. 3). (Fig. A7 in Appendix). ~~The average value of~~  $A_{fruit}$  is around 1 (relative to total vegetative allocation), ~~resulting nearly half of available assimilates allocated to the fruit pool and the rest to the vegetative pools.~~

An important allocation strategy for leaf is the division of displayed versus storage pools according to the before-introduced pre-expansion and post-expansion phenological phases. These two types of leaf C and N pools are distinct in that only the displayed pools contribute to LAI growth, whereas the storage pools support the growth of unexpanded phytomers, i.e. bud & spear leaves, which remain photosynthetically inactive. Total C and N allocation to the overall leaf pool (Eqs. A2 and A5) is divided to the displayed and storage pools by a fraction  $lf_{disp}$  (Table 2) according to the following equation:

$$\frac{A_{leaf}^{display}}{A_{leaf}^{storage}} = \frac{lf_{disp} \times A_{leaf}}{(1 - lf_{disp}) \times A_{leaf}} \quad (\text{Eq. 3})$$

The leaf storage here is only intended to differentiate the pre-expansion (negative ranks, photosynthetically inactive) and post-expansion (positive ranks, photosynthetically active) growth phases of leaves and is not used for supporting other tissues. These two phases and two types of pools coexist throughout oil palm's life at the PFT level, although at the sub-PFT level each phytomer only transits from one phase to another through time.

### 2.2.2. Sub-PFT level allocation

Total leaf and fruit allocations are partitioned to different phytomers, respectively, according to sub-PFT level allometry their phenological stages. Fruit allocation per phytomer is distributed to each phytomer using calculated with a sink size index:

$$S_p^{fruit} = \frac{GDD_{15} - H_p^{F.fill}}{H_p^{F.mat} - H_p^{F.fill}}, \quad (\text{Eq. 46})$$

where  $p$  stands for the phytomer number,  $H_p^{F.fill}$  and  $H_p^{F.mat}$  are the phenological indices for the start of fruit-fill and fruit maturity (with where  $H_p^{F.fill} \leq GDD_{15} \leq H_p^{F.mat}$ ).  $S_p^{fruit}$

increases from zero at the beginning of fruit-fill to the maximum of 1 right before harvest for each phytomer. This is because the oil palm fruit accumulates assimilates at increasing rate

during development until the peak when it becomes ripe and oil synthesis dominates the demand (Corley and Tinker, 2003). The sum of  $S_p^{fruit}$  for all phytomers gives the total reproductive sink size index, ~~which fluctuates according to the number of phytomers and their phenological cycles~~. Each phytomer receives a portion of fruit allocation by  $\frac{S_p^{fruit}}{\sum_{p=1}^n S_p^{fruit}} \times A_{fruit}$ , where  $A_{fruit}$  is the overall fruit allocation by Eq. 25.

An important allocation strategy for leaf is the division of displayed versus storage pools for the pre-expansion and post-expansion leaf growth phases. These two types of leaf C and N pools are distinct in that only the displayed pools contribute to LAI growth, whereas the storage pools support the growth of unexpanded phytomers, i.e. bud & spear leaves, which remain photosynthetically inactive. Total C and N allocation to the overall leaf pool is divided to the displayed and storage pools by a fraction  $lf_{disp}$  (Table A2) according to the following equation:

$$\begin{aligned} A_{leaf}^{display} &= lf_{disp} \times A_{leaf} \\ A_{leaf}^{storage} &= (1 - lf_{disp}) \times A_{leaf} \end{aligned} \quad (Eq. 7)$$

The plant level  $A_{leaf}^{display}$  and  $A_{leaf}^{storage}$  are then ~~Real-time leaf allocations to the displayed and storage pools are~~ distributed evenly to expanded and unexpanded phytomers, respectively, at each time step. When a phytomer enters the expansion phase, C and N from its leaf storage pools transfer gradually to the displayed pools during the expansion period. Therefore, a transfer flux is added to the real-time allocation flux and they together contribute to the post-expansion leaf growth.

LAI is calculated only for each expanded phytomer according to a constant specific leaf area (SLA, ~~Table 2~~) and prognostic amount of leaf C accumulated by phytomer  $n$ . In case it reaches the prescribed maximum ( $PLAI_{max}$ ), partitioning of leaf C and N allocation to this phytomer becomes zero.

### 2.3. Other parameterizations

Nitrogen retranslocation is performed exclusively during leaf senescence and stem turnover.

A part of N from senescent leaves and from the portion of live stem that turns to dead is

remobilized to a separate N pool that feeds plant growth or reproductive demand (~~section~~

~~2.1.6~~). Nitrogen of fine roots is all moved to the litter pool during root turnover. We do not

consider N retranslocation from live leaves, stem and roots specifically during grain-fill that

is designed for annual crops, ~~which in effect turns the N contents in all vegetative parts to~~

~~levels similar to crop residues in order to meet organ demand~~ (Drewniak et al., 2013).

~~because. For oil palm has continuous fruit-fill, once fruit fill starts it continues~~ year around

at different phytomers. ~~All the vegetative components have to be sustained at the same time.~~

~~Therefore, it is not reasonable to drain N from live leaves, stem and roots for the continuous~~

~~fruit filling.~~

The fertilization scheme for oil palm is also adapted to the plantation management in our

study area, which applies fertilizer biannually, only since 6-year old after planting, assuming

each fertilization event lasts one day. Currently the CLM-CN belowground routine CLM4.5

~~model~~ uses an unrealistically high denitrification rate, which results in a 50% loss of the

unused available soil mineral nitrogen each day under conditions of excess N (Oleson et al.,

2013). This caused ~~the our~~ simple biannual regular fertilization nearly useless because peak N

demand by oil palm is hard to predict given its continuous fruiting and vegetative growth and

most fertilized N is thus lost in several days. The high denitrification parameterization has

been recognized as an artifact (Drewniak et al., 2013; Tang et al., 2013). According to a study

on a banana plantation in the tropics (Veldkamp and Keller, 1997), around 8.5% of fertilized

N is lost as nitrogen oxide ( $N_2O$  and  $NO$ ). Accounting additionally for a larger amount of

denitrification loss to gaseous  $N_2$ , we modified the daily denitrification rate from 0.5 to 0.001,

which gives a 30% annual loss of N due to denitrification that matches global observations

(Galloway et al., 2004).



The irrigation option is turned off because oil palm plantations in the study area are usually not irrigated. ~~The vegetative structure is updated for oil palm including a special calculation of stem area index (SAI) and canopy top and bottom height allometry (Table B1 in Appendix), which are involved in biophysical processes in CLM model (Fig. 2).~~ Other input parameters for the new oil palm PFT such as its optical, morphological, and physiological characteristics are ~~estimated based on a literature review and field observations (summarized in Table B1A3).~~ Most of them are generalized over the life of oil palm.

### 3. Model evaluation

#### 3.1. Site data

Two oil palm plantations in the Jambi province of Sumatra, Indonesia provide data for calibration. One is a mature industrial plantation at PTPN-VI (01 °41.6' S, 103 °23.5' E, 2186 ha) planted in 2002, which provides long-term monthly harvest data (2005 to 2014) ~~to compare with model simulated yield~~. Another is a 2-year young plantation at a nearby smallholder site Pompa Air (01 °50.1' S, 103 °17.7' E, 5.7 ha). The leaf area and dry weight at multiple growth stages were measured by sampling leaflets of phytomers at different ranks (+1 to +20) on a palm and repeating for 3 different ages within the two plantations, ~~which were used to calibrate the model for simulating LAI development~~. The input parameter SLA (Table A2) was derived from leaf area and dry weight (excluding the heavy rachis). The phytomer-level LAI was estimated based on the average number of leaflets (90-300) per leaf of a certain rank and the PFT-level LAI was estimated by the average number of expanded leaves (35-45) per palm of a certain age. In both cases, a planting density of 156 palms per hectare (8m × 8m per palm) was used according to observation.

Additionally, LAI, yield and NPP independent leaf ~~measurements and yield data~~ from eight independent smallholder oil palm plantations sites (50m × 50m each) were used for model validation. Four of these sites (HO1, HO2, HO3, HO4) are located in the Harapan region

nearby PTPN-VI, and another four (BO2, BO3, BO4, BO5) are located in Bukit Duabelas  
 region (02 °04' S, 102 °47' E), both in Jambi, Sumatra. ~~Leaf area and dry weight and SLA of~~  
~~whole leaf samples were measured for different sites. They were converted to LAI as above.~~  
~~Oil palm~~ Fresh bunch harvest data were collected at these sites for a whole year ~~from July~~  
~~2013 to July~~in 2014. Harvest records from both PTPN-VI and the 8 validation sites were  
 converted to harvested carbon ( $\text{g C/m}^2$ ) with mean wet/dry weight ratio of 58.65 % and C  
 content 60.13 % per dry weight according to C:N analysis (Kotowska et al., 2015). The oil  
palm monthly NPP and its partitioning between fruit, leaf, stem and root were estimated  
based on measurements of fruit yield (monthly), pruned leaves (monthly), stem increment  
(every 6 month) and fine root samples (once in a interval of 6-8 month) at the eight validation  
sites (Kotowska et al., 2015b).

The amount of fertilization at the industrial plantation PTPN-VI was  $456 \text{ kg N ha}^{-1} \text{ yr}^{-1}$ ,  
applied regularly twice per year since 6-year old. The smallholder plantations in Harapan (H  
plots) and Bukit Duabelas (B plots) used much less fertilizer. From interview data, the H plots  
had roughly regular N fertilization (twice per year), whereas among the B plots only BO3  
indicated one fertilization event per year but the amount was unclear (applied chicken manure  
in 2013) and the other plots had no N fertilization in 2013 and 2014 due to financial difficulty.  
Fertilization history prior to 2013 is unavailable for all the smallholder plantations. Given the  
limited information, we consider two levels of fertilization for H plots (regular:  $96 \text{ kg N ha}^{-1}$   
 $\text{yr}^{-1}$ , from 6-year old until 2014) and B plots (reduced:  $24 \text{ kg N ha}^{-1} \text{ yr}^{-1}$ , from 6-year old until  
2012), respectively.

The mean annual rainfall (the Worldclim database: <http://www.worldclim.org> (Hijmans et al.,  
 2005); average of 50 years) of the two investigated landscapes in Jambi Province was  $\sim 2567$   
 $\text{mm y}^{-1}$  in the Harapan region (including PTPN-VI) and  $\sim 2902 \text{ mm y}^{-1}$  in the Bukit Duabelas  
 region. In both areas, May to September represented a markedly drier season in comparison to  
 the rainy season between October and April. Air temperature is relatively constant throughout

the year with an annual average of 26.7 °C. In both landscapes, the principal soil types are Acrisols: in the Harapan landscape loam Acrisols dominate, whereas in Bukit Duabelas the majority is clay Acrisol. Soil texture such as sand/silt/clay ratios and soil organic matter C content were measured at multiply soil layers (down to 2.5m) (Allen et al., in review). They were used to create two sets of surface input data for the ~~Harapan (H) and Bukit Duabelas (B)~~two regions separately.

### 3.2. Model setup

The model modifications and parameterizations ~~are~~were implemented according to CLM~~4.5~~ standards. A new sub-PFT dimension called *phytomer* ~~is~~was added to all the new variables so that the model can output history tapes of their values for each phytomer and prepare restart files for model stop and restart with bit-for-bit continuity. Simulations were set up in point mode (a single 0.5×0.5 degree grid) at every 30-min time step. A spin-up procedure (Koven et al., 2013) was followed to get a steady-state estimate of soil C and N pools, with the CLM-CN decomposition cascade and broadleaf evergreen tropical forest PFT. The soil C and N pools were rescaled to match the average field observation at two reference lowland rainforest sites in Harapan and Bukit Duabelas regions (Allen et al., 2015; Guillaume et al., 2015), which serve as the initial conditions. The forest was replaced with the oil palm at a specific year of plantation establishment (2002 for PTPN-VI and 1996, 1997, 1999, 2000, 2001, 2002, 2003, 2004 for HO3, HO1, HO2, BO2, BO3, BO4, HO4, BO5, respectively). The oil palm functions were then turned on and simulations continued until 2014. The 3-hourly ERA Interim climate data (Dee et al., 2011) were used as atmospheric forcing.

~~Simulations were set up in point mode (a single 0.5×0.5 degree grid) at every 30-min time step. Atmospheric forcing data from the CRU-NCEP global reanalysis dataset (Viovy, 2011) were interpolated to the PTPN-VI site for model spin-up. The soil texture measurements in the Harapan region together with other surface conditions from global dataset were used as surface input. The test point was initially prescribed with 100% broadleaf evergreen tropical~~

forest PFT that existed before 1850. A 600-year accelerated spin-up procedure (Koven et al., 2013) was performed till 1850 with constant CO<sub>2</sub> and nitrogen deposition to get a steady-state estimate of soil C and N pools. Simulation continued on this equilibrium condition but was forced with dynamic CO<sub>2</sub> and NCEP meteorological data until 1990. Restart files from 1990 were used as soil initial condition for the following simulations.

The surface was then replaced with 100% oil palm PFT, while the soil C and N pools were maintained from the initial condition. The new sub-canopy phytomer structure, phenology and allocation schemes were turned on. Recent simulations were all forced with dynamic CO<sub>2</sub> and 3-hourly ERA Interim reanalysis atmospheric data until 2014 (Dee et al., 2011). Input meteorological variables include surface incident solar radiation (FSDS), surface incident longwave radiation (FLDS), 2-meter temperature (TBOT), precipitation rate (PRECTmms), 10-meter wind (WIND), 2-meter dewpoint temperature (TDEW, in place of relative humidity), surface pressure (PSRF).

A simulation from 2002 to 2014 at the PTPN-VI site was used for model calibration. Additional eight simulations were run for the sites HO1, HO2, HO3, HO4, BO2, BO3, BO4, BO5 with different surface input files (for soil texture) and different atmospheric forcing files for the H and B plots, respectively. The simulations started from different years (1996, 1997, 1999, 2000, 2001, 2002, 2003, 2004) when the palms were planted at the individual sites. Outputs from these simulations were used to validate the model in terms of LAI and yield.

### 3.3. Calibration of key parameters

A simulation from 2002 to 2014 at the PTPN-VI site was used for model calibration. Both the PFT level and phytomer level LAI development were calibrated with field observations in 2014 from a chronosequence approach (space for time substitution) using oil palm samples of three different age and multiple phytomers of different rank (section 3.1). Simulated yield outputs (around twice per month) were calibrated with monthly harvest records of PTPN-VI

plantation from 2005 to 2014. Cumulative yields were compared because the timing of harvest in the plantations was largely uncertain and varied depending on weather and other conditions.

To simplify model calibration, we focused on parameters related to the new phenology and allocation processes. Phenological parameters listed in Table A1 were determined according to field observations and existing knowledge about oil palm growth phenology (Combres et al., 2013; Corley and Tinker, 2003) as well as plantation management in Sumatra, Indonesia. Allocation coefficients in Table A2 were more uncertain and they were the key parameters to optimize in order to match observed LAI and yield dynamics according to the following sensitivity analysis. Measurements of oil palm NPP and its partitioning between fruit, canopy, stem, and root from the eight sites (section 3.1 Kotowska et al., 2015) were used as a general reference when calibrating the allocation coefficients.

Leaf C:N ratio and SLA were determined by field measurements. Other C:N ratios and optical and morphological parameters in Table A3 were either fixed by field observations or adjusted in-between trees and crops. Parameters related to photosynthesis, stomatal conductance and respirations were set at similar levels as those of other crops, except that leaf traits such as  $PLAI_{max}$  and SLA were determined by field measurements. Other parameters such as C:N ratios of the leaf, stem, root and fruit components were also left as similar levels as other crop PFTs.

### 3.4. Sensitivity analysis

Performing a full sensitivity analysis of all parameters used in simulating oil palm (more than 100 parameters, though a majority are shared with natural vegetation and other crops) would be a challenging work. As with calibration, we limited the sensitivity analysis to a set of parameters introduced for the specific PFT and model structure designed for oil palm (Tables A1 and A2). Among the phenological parameters, *mxlivenp* and *phyllochron* are closely

related to pruning frequency (section 2.1.6) but they should not vary widely for a given oil palm breed and plantation condition. Therefore, they were fixed at the average level for the study sites in Jambi, Sumatra (Table 1). Parameter  $PLAI_{max}$  is only meant for error controlling, although in our simulations phytomer-level LAI never reached  $PLAI_{max}$  (see Fig. 5 Fig. 4 in results) because environmental constraints and nitrogen down-regulation already limited phytomer leaf growth well within the range.  $GDD_{init}$  was kept zero because only the transplanting scenario was considered for seedling establishment.

We tested two hypotheses of phytomer level leaf development based on the other phenological parameters: 1) considering the leaf storage growth period, that is, the bud & spear leaf phase is explicitly simulated with the GDD parameter values in Table A1 and  $lf_{disp} = 0.3$  in Table A2; 2) excluding the storage growth period by setting  $GDD_{exp} = 0$  and  $lf_{disp} = 1$  so that leaf expands immediately after initiation and leaf C and N allocation all goes to the photosynthetic active pools.

The sensitivity of allocation and photosynthesis parameters in Table A2 were tested by adding or subtracting 10% or 30% to the baseline values (calibrated) one-by-one and calculating their effect on final cumulative yield at the end of simulation (December 2014). In fact, all the allocation parameters are interconnected because they co-determine photosynthesis capacity and respiration costs as partitioning to the different vegetative and reproductive components varies. This simple approach provides a starting point to identify sensitive parameters, although a more sophisticated sensitivity analysis is needed in the future effort.

~~Parameter  $PLAI_{max}$  is only meant for error controlling, although in our simulations phytomer-level LAI never reached  $PLAI_{max}$  (see Fig. 4 in results) because environmental constraints and nitrogen down-regulation already limited phytomer leaf growth well within the range. Therefore, this parameter was not analyzed for its sensitivity. The C:N ratios and some photosynthesis and respiration parameters (Table A1) were evaluated thoroughly in Bilionis et al. (2015). Since we do not consider specific N retranslocation during fruit fill, some C:N~~

~~parameters are not used for oil palm and the aspect of N content in different plant tissues is not prioritized for this sensitivity analysis.~~

### 3.5. Validation

In this study, we only validated the model structure and model behavior on simulating aboveground C ~~dynamics and~~ partitioning ~~and flux~~ as represented by LAI ~~and~~ fruit yield ~~and~~ NPP. Independent ~~leaf measurement, yield and monthly NPP LAI and yield~~ data collected in ~~2013–~~2014 from the eight mature oil palm sites (H and B plots) ~~different sites~~ were compared with ~~model predictions from~~ eight simulations using the above same model setting and calibrated parameters, except that two categories of climate forcing, surface input data (for soil texture) and fertilization (regular vs. reduced) were prescribed for the H plots and B plots, respectively.

## 4. Results

### 4.1. Calibration with LAI and yield

In model calibration with the industrial PTPN-VI plantation, the PFT-level LAI dynamics simulated by the model incorporating the pre-expansion phase matches well with the LAI measurements for three different ages (Fig. 34). Simulated LAI for the PFT increases with age in a sigmoid relationship. The dynamics of LAI is also impacted by pruning and harvest events because oil palms invest around half of their assimilates into fruit yield. Oil palms are routinely pruned by farmers to maintain the maximum number of expanded leaves around 40. Hence, when yield begins 2-3 years after planting, LAI recurrently shows an immediate drop after pruning and then quickly recovers. The pruning frequency decreases with age because the phyllochron increases to 1.5 times at 10-year old (Supplementary materials). Simulations without the pre-expansion storage growth phase show an unrealistic fast increase of LAI before 3 years old, much higher than observed in the field. At older age after yield begins, LAI drops drastically and recovers afterwards. Although the final LAI could stabilize at a

similar level, the initial jump and drop of LAI at young stage do not match field observations and cannot be solved by adjusting parameters other than  $GDD_{exp}$ . Hereafter, the following simulations were all run using the pre-expansion phase.

The phytomer level LAI development ~~also matches well~~ is comparable with leaf samples from the field measurements (Fig. 45). The two leaf samples at rank 5 (LAI = 0.085) and rank 20 (LAI = 0.122) of a mature oil palm in PTPN-VI (the two black triangles for 2014) are within the range of simulated values. The other sample at rank 25 (LAI = 0.04; in 2004 section of Fig. 4) on a young oil palm in Pompa Air (smallholder plantation) is slightly lower than the simulated value. ~~This sub-PFT level LAI dynamics~~ Each horizontal color bar clearly marks the ~~6-phase~~ post-expansion leaf phenology cycle, including gradual increment during phytomer development and gradual declining during senescence. ~~The figure only shows photosynthetic LAI that updates at every time step. Leaf C accumulation before leaf expansion~~ The pre-expansion phase is not ~~shown~~ included here in the figure but model outputs show that roughly 60-70% of leaf C in a phytomer is accumulated before leaf expansion, which is co-determined by the allocation ratio  $lf_{disp}$  and the lengths of two growth phases set by  $GDD_{exp}$  and  $GDD_{L_{mat}}$ . This is comparable to observations on coconut palm that dry mass of the oldest unexpanded leaf accounts for 60% of that of a mature leaf (Navarro et al., 2008). Only when the palm becomes mature, phytomer LAI could come closer to the prescribed  $PLAI_{max}$  (0.165). However, during the whole growth period from 2002 to 2014 none of the phytomers have reached  $PLAI_{max}$ , which is the prognostic result of the carbon balance simulated by the model.

The cumulative yield of baseline simulation has overall high consistency with harvest records (Fig. 56). The mean percentage error (MPE) is only 4%. The slope of simulated curve increases slightly after 2008 when the LAI continues to increase and NPP reaches a high level (Fig. A73). The harvest records also show the same pattern after 2008 when heavy fertilization began (456 kg N/ha/yr). ~~If a high denitrification rate is used, fertilization becomes~~



~~useless even given the already high dosage and the plant cannot catch up with observation after 2009.~~

~~Comparing the monthly trend of yield (Fig. 6),~~ The per-month harvest records exhibit strong zig-zag pattern (Fig. 7). One reason is that oil palms are harvested every 15-20 days and summarizing harvest events by calendar month would result in uneven harvest times per month, e.g. two harvests fall in a previous month and only one in the next month. ~~It would be more appropriate to use yield data per harvest event to compare with model output.~~ Yet it still shows that harvests at PTPN-VI plantation dominated from October to December whereas in the earlier months of each year harvest amounts were significantly lower. The simulated ~~amount of monthly~~ yield ~~per harvest event~~ has less seasonal fluctuation, but it responds to the drought periods (Fig. 6). A positive linear correlation exists between simulated yield and the mean precipitation of a 60-day period (corresponds to the main fruit-filling and oil synthesis period) before each harvest event (Pearson's  $r = 0.15$ ). Examining the longer term year-to-year variability, a clear increasing trend of yield with increasing plantation age is captured by the model, largely matching field records since the plantation began to yield in 2005.

## 4.2. Sensitivity analysis

The leaf nitrogen fraction in Rubisco ( $F_{LNR}$ ) is shown to be the most sensitive parameter (Fig. 7), because it determines the maximum rate of carboxylation at 25 °C ( $V_{cmax25}$ ) together with  $SLA$  (also sensitive), foliage nitrogen concentration ( $CN_{leaf}$ , Table B1A3) and other constants. Given the fact that  $F_{LNR}$  should not vary widely in nature for a specific plant, we constrained this parameter within narrow boundaries to give a  $V_{cmax25}$  around 100.7, ~~which is similar to the same as~~ that shared by all other crop PFTs ~~(100.7) and higher than forests (around 60)~~ in CLM. We fixed  $SLA$  (to 0.013) ~~was fixed~~ by field measurements. The value is only representative of the photosynthetic leaflets. ~~The heavy rachis that supports leaflets is about 75% of the weight of a whole phytomer and contains a large proportion of lignified tissue (Corley and Tinker, 2003). Thus, the rachises are considered as a part of the stem-like tree~~

~~branches and included in stem turnover, which reduces respiration cost compared to when it is~~  
~~maintained as a part of the metabolically active leaf. However, bias could exist as the~~  
~~physiology of rachis esp. during the juvenile phase of bud & spear leaf is likely very different~~  
~~from stem. We use this parameterization because it fits the structure of the CLM model.~~ The  
 initial root allocation ratio ( $a_{root}^i$ ) has significant influence on yield because it modifies the  
 overall respiration cost along the gradual declining trend of fine root growth across 25 years  
 (Eqs. ~~1A1, A4~~). The final ratio ( $a_{root}^f$ ) has limited effects because its baseline value (0.1) is  
 set very low and thus the percentage changes are insignificant. The leaf allocation coefficients  
 ( $f_{leaf}^i, a_{leaf}^f$ ) are very sensitive parameters because they determine the magnitudes of LAI  
 and GPP and consequently yield. The coefficients  $d_{mat}$  and  $d_{alloc}^{leaf}$  control the nonlinear curve  
 of leaf development (Eq. ~~A54~~) and hence the dynamics of NPP and that partitioned to fruits.  
~~They were calibrated to match both the LAI and yield dynamics.~~ Increased  $F_{stem}^{live}$  results in  
 higher proportion of live stem throughout life, given the fixed stem turnover rate (~~section~~  
~~2.1.7 Supplementary materials~~), and therefore it brings higher respiration cost and lower yield.  
~~Decreasing the fruit allocation coefficient  $a$  results in a higher base rate of  $A_{fruit}$  according to~~  
~~Eq. 2, whereas increasing coefficient  $b$  brings up the rate of change and final magnitude of~~  
 ~~$A_{fruit}$  if NPP rises continuously.~~ Their relative influence of fruit allocation coefficients  $a$  and  
 $b$  on yield is much lower than the leaf allocation coefficients because of the restriction of  
 ~~$A_{fruit}$~~  by NPP dynamics (Eq. ~~25~~, Fig. ~~A73~~). Parameters  $lf_{disp}$  and *transplant* have negligible  
 effects.  $lf_{disp}$  has to work together with the phenological parameter  $GDD_{exp}$  to give a  
 reasonable size of spear leaf ~~vesf~~ before expansion according to field observation (~~section 5.2~~).  
The sensitivity of  $GDD_{exp}$  is shown in Fig. 4. Varying the size of seedlings at transplanting by  
 10% or 30% does not alter the final yield, likely because the ~~resulting~~ initial LAI is still  
 within a limited range (0.1~0.2) given the baseline value 0.15.

### 4.3. Model validation with independent dataset

The LAI development curves for the eight oil palm sites follow similar patterns since field transplanting in different years, except that the B plots (BO2, BO3, BO4) are restrained in LAI growth after 11 years old because of reduced fertilization (Fig. 9a). The field data in 2014 also shows the check by N limitation and even exhibits a decreasing trend of LAI with increasing plantation age at B plots except BO5 which is under 10 years old (Fig. 9b). In general, the modelled LAI has a positive relationship with plantation age under regularly fertilized condition and it stabilizes after 15-year old (site HO3) as controlled by  $d_{mat}$  (Eq. 4). This age-dependent trend is observed in the field with a notable deviation by site HO1. The average LAI of the eight sites from the model is comparable with field measurement in 2014 (MPE = 13%). There are large uncertainties in field LAI estimates because we did not measure LAI at the plot level directly but only sampled leaf area and dry weight of individual phytomers and scaled the values up. (Fig. 8a). The final LAIs at 2014 match poorly with observations at each individual site, but the average LAI values between simulations and field measurements are comparable (MPE = 10%) (Fig. 8b). There is large uncertainty in field LAI estimates because we did not directly measure LAI at the plot level but only sampled leaf area and dry weight of individual phytomers. Plantation management is also very different between these 8 smallholder plantations. For example, H plots applied significantly higher fertilization than B plots, while the model prescribes the same fertilization for all plots (section 2.3).

The simulated annual yields match closely with field observations in 2014 at both the H plots (MPE = 2%) and B plots (MPE = 2%; Fig. 10). With regular fertilization in the H plots, both the modelled and observed yield are slightly higher in the older plantations (HO2, HO1, and HO3) than the younger one (H04) but stabilize around  $1280 \text{ g C m}^{-2} \text{ yr}^{-1}$  past the age of 15 years. In contrast, the B plots have significantly lower yield because of reduced N input and the model is able to capture the N limitation effect on both NPP and yield, i.e. the declining trend with increasing age, which is consistent with field observation. The model simulates slightly higher NPP than field estimates at 7 smallholder sites (MPE = 10%) using the input

parameters calibrated and optimized only for LAI and yield at the industrial PTPN-VI plantation. Field measured leaf NPP only includes leaf litter production but does not account for the growing size of canopy (i.e. increasing LAI).

~~The simulated annual yields match closely with the average yield of the eight sites measured in 2013-2014 (MPE = -4%) but the model predicted variability across the sites is much lower than field records (Fig. 9). Modelled yield generally increases with plantation age, which can be explained by the increasing fruit allocation rate  $A_{fruit}$  with increasing LAI and NPP (Fig. A7). We do not have data to test an aging decline function of growth and yield and assume the oil palm plantations remain productive for 25 years ( $Age_{max}$ ) before replanting. Site-to-site variation in the field harvest data is still difficult to interpret, because the measured yields do not correlate with age and LAI measurements, possibly reflecting unknown differences in fertilization or other management practices.~~

~~Overall, the simulated LAI and yield seem reasonable on an average, but has smaller site-to-site variability than observation as fertilization and other management impacts were set constant in the model.~~

## **5. Discussion**

Calibration and validation with multiple site data demonstrate the ~~functionality~~ utility of CLM-Palm ~~the new PFT~~ and its sub-canopy structure for simulating the growth and yield of the unique oil palm plantation system within a land surface modeling context.

The pre-expansion phenological phase is proved necessary for simulating both phytomer-level and PFT-level LAI development in a prognostic manner. The leaf C storage pool provides an efficient buffer to support phytomer development and maintain overall LAI during fruiting. It also avoids an abnormally fast increase of LAI in the juvenile stage when C and N allocation is dedicated to the vegetative components. Without the leaf storage pool, the plant's canopy develops unrealistically fast at young age and then enters an emergent drop

once fruit-fill begins (Fig. 4). This is because the plant becomes unable to sustain leaf growth just from its current photosynthetic assimilates when a large portion is allocated to fruits.

The model well simulates year-to-year variability in yield (Fig. 7), in which the increasing trend is closely related to the fruit allocation function (Fig. 3) and LAI development (Fig. 4). The seasonal variability in simulated yield corresponds to the precipitation data but it is difficult to interpret the difference with monthly harvest records due to the artificial zig-zag pattern. The harvest records from plantations do not necessarily correspond to the amount of mature fruits along a phenological time scale due to varying harvest arrangements, e.g. fruits are not necessarily harvested when they are ideal for harvest, but when it is convenient. Observations of mature fruits on a tree basis (e.g. Navarro et al., 2008 on coconut) would be more suitable to compare with modeled yield, but such data are not available at our sites. Some studies have also demonstrated important physiological mechanisms on oil palm yield including inflorescence gender determination and abortion rates that both respond to seasonal climatic dynamics although with a time lag (Combres et al., 2013; Legros et al., 2009). The lack of representation of such physiological traits might affect the seasonal dynamics of yield simulated by our model, but these mechanisms are rarely considered in a land surface modelling context. Nevertheless, the results correspond generally to the purpose of our modelling which is focused on the long-term climatological effects of oil palm agriculture. The correct representation of multi-year trend of carbon balance which we did reach is more important than the correct prediction of each yield. For latter the more agriculturally-oriented models should be used.

Resource allocation patterns for perennial crops are more difficult to simulate than annual crops. For annuals, the LAI is often assumed to decline during grain-fill (Levis et al., 2012). However, the oil palm has to sustain a rather stable leaf area while partitioning a significant amount of C to the fruits. The balance between reproductive and vegetative allocations is crucial. The dynamics of  $A_{fruit}$  as a function of monthly NPP is proved useful to capture the

881 increasing yield capacity of oil palms during maturing at favorable conditions (Fig. 6, 7) and  
882 also able to adjust fruit allocation and shift resources to the vegetative components under  
883 stress conditions (e.g. N limitation, Fig. 9 and 10). The value of  $A_{fruit}$  increased from 0.5 to  
884 1.5 (Fig. 3), resulting more than a half partitioning of NPP to the reproductive pool at mature  
885 stage which matched closely with field observations (Fig. 10; Kotowska et al., 2015a;  
886 Kotowska et al., 2015b). Our experiments (not shown here) confirmed that the dynamic  
887 function is more robust than a simple time-dependent or vegetation-size-dependent allocation  
888 function.

889 The phenology and allocation processes in land surface models are usually aimed to represent  
890 the average growth trend of a PFT at large spatial scale (Bonan et al., 2002; Drewniak et al.,  
891 2013). We made a step forward by comparing point simulations with multiple specific site  
892 observations. The model predicts well the average LAI development and yield as well as NPP  
893 of mature plantations across two different regions. Site-to-site variability in yield and NPP at  
894 the Harapan and Bukit Duabelas plots under contrasting conditions (regular vs. reduced  
895 fertilization) is largely captured by the model. The decreasing trend of yield and pause of LAI  
896 growth in B plots after 10 years old (Fig. 9, 10) reflect reduced N availability observed in the  
897 clay Acrisol soil in Bukit Duabelas (Allen et al., 2015) with very limited C and N return from  
898 leaf litter because of pruning and piling of highly lignified leaves (Guillaume et al., 2015).  
899 Yet there remains small-scale discrepancy in LAI, NPP or yield in some sites which is  
900 possibly due to the fact that microclimate, surface input data and the amount and timing of  
901 fertilization were only prescribed as two categories for H and P plots, respectively. Field data  
902 show the proportion of NPP allocated to yield is significantly higher in plot HO1 (70%) than  
903 in other plots (50% to 65%) which could explain the low LAI of HO1. This is not reflected in  
904 the model as the same parameters are used in the fruit allocation function (Eq. 5) across sites.  
905 The deviation in allocation pattern is likely due to difference in plantation management (e.g.  
906 harvest and pruning cycles), which has been shown to be crucial for determining vegetative  
907 and reproductive growth (Euler et al., 2015). Other factors such as insects, fungal infection,

and possibly different oil palm progenies could also result in difference in oil palm growth and productivity, but they are typically omitted in land surface models. Generalized input parameterization across a region is usually the case when modeling with a PFT, although a more complex management (e.g. dynamic fertilization) scheme could be devised and evaluated thoroughly with additional field data, which we lack at the moment.

Overall, the sub-canopy phytomer-based structure, the extended phenological phases for a perennial crop PFT and the two-step allocation scheme of CLM-Palm are distinct from existing functions in land surface models. The phytomer configuration is similar to the one already implemented in other oil palm growth and yield models such as the APSIM-Oil Palm model (Huth et al., 2014) or the ECOPALM yield prediction model (Combres et al., 2013). But the implementation of this sub-canopy structure is the first attempt among land surface models. CLM-Palm incorporates the ability of an agricultural model for simulating growth and yield, beside that it allows the modeling of biophysical and biogeochemical processes as a land model should do, e.g. what is the whole fate of carbon in plant, soil and atmosphere if land surface composition shifts from a natural system to the managed oil palm system? In a following study, a fuller picture of the carbon, nitrogen, water and energy fluxes over the oil palm landscape are examined with CLM-Palm presented here and evaluated with Eddy Covariance flux observation data. We develop this palm sub-model in the CLM framework as it allows coupling with climate models so that the feedbacks of oil palm expansion to climate can be simulated in future steps.

~~Results showed a limitation of the model, that is, the difficulty to capture the large site-to-site variation in yield and LAI. The discrepancy was very likely due to insufficient representation of management (e.g. fertilization, harvest cycle) in the model, which has been shown to be crucial for determining oil palm growth and yield (Euler et al., in review). Field observations in the 8 smallholder plots (B and H plots) show that increased harvest cycle decreases yield because of fruit respiration costs. Other factors such as pruning, soil conditions (only two~~

categories for H and B plots) and possibly different oil palm progenies could also result in difference in the average size and number of leaves and fruits per palm, but the model uses uniform parameterization of these aspects across sites. Especially the amount and timing of fertilization vary largely from plantation to plantation and from year to year. Thus a more complex dynamic fertilization scheme needs to be devised and evaluated thoroughly (together with the new denitrification rate) with additional field data, which we lack at the moment. The seasonal variability in yield simulated by the model well corresponds to precipitation data but it is difficult to interpret the difference with harvest records due to the artificial zig-zag pattern. Moreover, the harvest records from plantations do not necessarily correspond to the amount of mature fruits along a phenological time scale due to varying harvest arrangements, e.g. fruits are not necessarily harvested when they are ideal for harvest, but when it is convenient. Observations of mature fruits on a tree basis would be more suitable to compare with modeled yield, but such data are not available. Some studies have also demonstrated important physiological mechanisms on oil palm yield including inflorescence gender determination and abortion rates that both respond to seasonal climatic dynamics although with a time lag (Combres et al., 2013; Legros et al., 2009). The lack of representation of such physiological traits might affect the seasonal dynamics of yield simulated by our model, although these mechanisms are rarely considered in a land surface modelling context.

Nevertheless, the multilayer phytomer based structure, the extended phenological phases for a perennial crop PFT and the two-step allocation scheme are distinct from existing functions in land models. Their significance and implications as shown in the results are discussed below. In the future, a fuller picture of the carbon, water and energy fluxes over the oil palm landscape will be examined with the oil palm module presented here and be evaluated with Eddy Covariance flux observation data.

## 5.1 The unique phenological phase for leaf storage growth



The pre-expansion growth phase is proved necessary for simulating phytomer leaf growth and PFT LAI in a prognostic manner within the CLM framework. Real time allocation of assimilates to the leaf C pool is depending on incoming solar energy, N availability and other environmental forcing variables. In our model implementation, the leaf C storage pool accumulated by each phytomer during its bud & spear leaf stage is released gradually, which comes together with the real time leaf C allocation, to support the increment of photosynthetic active leaf C pool within the leaf expansion period. Therefore, the storage growth period and abundant storage C pool provides an efficient buffer to support phytomer development and maintain overall LAI when resources are limited during fruit fill or environmental constraints. It also avoids an abnormally fast increase of LAI in the young palms before fruiting when C and N allocation is dedicated to the vegetative components. Without the leaf storage pool, the plant's canopy develops unrealistically fast at young age and then enters an emergent drop once fruit fill begins (Fig. 3). This is because the plant becomes unable to sustain leaf growth just from its current photosynthetic assimilates when a large portion is allocated to fruit, together with removal of leaf C by pruning.

The pre-expansion and post-expansion growth phases are usually not represented together in other studies. For example, the APSIM Oil Palm model (Huth et al., 2014) considers only post-expansion leaf growth for a period of 5 phyllochrons (~2 months) and it prescribes a logistic leaf area expansion pattern that is not constrained by assimilates supply. The ECOPalm model (Combres et al., 2013) assumes a 7 month leaf growth period with constant growth rate solely within the pre-expansion phase, that is, at negative ranks in bud & spear leaf stage. According to field observations, it is more realistic to include both pre-expansion and post-expansion growth for a phytomer to reach full vegetative maturity. Furthermore, differentiating the two contrasting phases of leaf growth could avoid abrupt increase in photosynthesis if a phytomer with full dry mass shifts from photosynthetically inactive to active status at one step. We implement the leaf senescence function for the similar purpose (section 2.1.6). The realistic parameterization of senescence differentiates the photosynthetic

capacity of a leaf at the bottom layer of canopy from those on the top so as to avoid unwanted drastic reduction in photosynthetic LAI that would happen if the bottom leaves were turned off immediately.

## 5.2 Allocation strategy

Allocation patterns for common annual crops are easier to simulate because their LAI is often assumed to decline during grain fill (Levis et al., 2012). However, perennial evergreen crops have to sustain a rather stable LAI while partitioning a significant amount of C to the grain or fruit component. How to balance reproductive and vegetative allocations is crucial. Oil palms in managed plantation remain productive year around for more than 25 years. If excessive allocation is given to yield without adjustment during resource limitation, it could eventually pull LAI down to a critical level when the plant cannot sustain vegetative maintenance and growth. The dynamics of  $A_{fruit}$  as a function of monthly NPP (Eq. 2) is meant to capture the increasing yield capacity of oil palms during maturing at favorable conditions (often the case in oil palm plantations). The average near 1:1 ratio to partition available assimilates to the reproductive and vegetative pools matched closely with field observations (Kotowska et al., 2015). In the simulations  $A_{fruit}$  increased rapidly from the base rate within one year after fruiting began, without impairing allocation for LAI development. This is because within the same period NPP also increased nearly 50% (Fig. A7). Correlating  $A_{fruit}$  with NPP thus matches the “overflow” model and follows ecophysiological evidence of source limitation of oil palm yield (Corley and Tinker, 2003). It avoids unrealistic increase of  $A_{fruit}$  under stressed conditions if a simple time-dependent or vegetative size-dependent fruit allocation function is used. When severe stress conditions do happen, this NPP-related function is expected to decrease fruit allocation and shifts resources to the vegetative components.

The pre-expansion phase is proved to be a crucial strategy that enables oil palm to maintain a stable LAI when a large ratio of reproductive allocation and leaf pruning are co-occurring.

We set the value of  $f_{disp}$  to be 0.3 for the post-expansion phase which means a majority of available C and N fluxes are allocated for storage growth. Together with the length of each growth phase set by  $GDD_{exp}$  and  $GDD_{L_{mat}}$ , they determine that roughly 60–70% of leaf C in a phytomer is accumulated before its expansion with the remaining part developed until leaf maturity. This is comparable to observations on coconut palm that dry mass of the oldest unexpanded leaf accounts for 60% of that of a mature leaf (Navarro et al., 2008).

### 5.3. The sub-canopy structure

We devised the sub-canopy structure for the phenology and allocation mechanisms in order to capture the growth and yield dynamics of the oil palm plantation system. Phytomer to-phytomer relationship is considered more “social” rather than independent (Corley and Tinker, 2003). In fact, oil palm fruit bunches are located at the lower ranks of the canopy while most photosynthesis happens on the top layers of young expanded phytomers which are exposed to more sunshine but not bearing fruits yet. This implies the young phytomers are more than self-sufficient and they share excessive photosynthetic products with older phytomers to support their fruit-fill demand. All the photosynthetic phytomers also support the storage growth of unexpanded phytomers that are in the bud & spear leaf stage, in addition to maintaining stem and root growths. Sharing a common pool of photosynthetic assimilates for C and N allocation also implies a competition among phytomers by their different demand levels at different phenological stages. Thus, the allocation ratios are demand-driven as controlled by phenology, whereas the actual allocation rates (in terms of gram C per second) are constrained by assimilates supply which is the result of climatic forcing, N down-regulation, and other environmental variables.

The sub-canopy structure could be also useful for considering light competition among expanded phytomers. However, in the current paper the CLM default one-layered sun/shade big-leaf canopy model is used for radiative transfer and photosynthesis, which is based on the two-stream approximation for an integrated canopy (Sellers, 1985). It also derives the sunlit

~~and shaded fractions for the whole canopy using an analytical solution by Dai et al. (2004), but the light profile is not resolved through the canopy depth. Thus, specific light competition among different phytomers and influence on their photosynthetic rates is not considered. But the sun shade canopy is a relevant and accurate simplification according to De Pury and Farquhar (1997) and Ryu et al. (2011). It has been cross validated with refined 3-D models on coconut palm by Roupsard et al. (2008). Calculating only canopy level photosynthesis is sufficient for the two step social sharing allocation strategy in which a common assimilates pool is partitioned to different phytomers regardless of the light profile.~~

~~Nevertheless, resolving light profile at sub canopy layers could possibly improve the accuracy of deriving canopy level photosynthesis and energy fluxes. A classical multilayer radiative transfer scheme by Norman (1979) and adapted photosynthesis calculations are currently incorporated into the CLM model as an option to work with the oil palm modules, allowing simulating sub canopy light profile.~~

## 6. Summary

The development of ~~the perennial oil palm~~ PFTCLM-Palm including its structure, phenology, and carbon and nitrogen allocation functions was proposed for modeling an important agricultural system ~~and land use transformation in Indonesiain the tropics~~. This paper demonstrates the ability of the new ~~oil~~ palm module to simulate the inter-annual dynamics of vegetative growth and fruit yield from field planting to full maturity of the plantation. The ~~multilayer canopy structure and associated sub-PFT level~~ sub-canopy-scale phenology and allocation strategy are necessary for this perennial evergreen crop which yields continuously on multiple phytomers. ~~They are potentially applicable to similar plantations (coconut palm, date palm, etc.).~~ The pre-expansion leaf storage growth phase is proved essential for buffering and balancing overall vegetative and reproductive growth. Average LAI yield and NPP are ~~and yield were~~ satisfactorily simulated for multiple sites, which fulfills the main mission of a land surface modeling approach, that is, to represent the average conditions and dynamics of

~~large-scale processes. On the other hand, simulating small-scale site-to-site variation (50m × 50m sites) requires detailed input data on site conditions (e.g. microclimate) and plantation managements that are often not available thus limiting the applicability of the model at small scale. Nevertheless, the CLM-Palm model sufficiently represents the significant region-wide variability in oil palm NPP and yield driven by nutrient input and plantation age in Jambi, Sumatra. and the model, designed initially to be run for large areas also proved to be attractive for point simulations, thanks to the overarching framework of the CLM model and the underlying ecophysiological processes that were introduced for oil palm.~~ The point simulations here provide a starting point for calibration and validation at large scales.

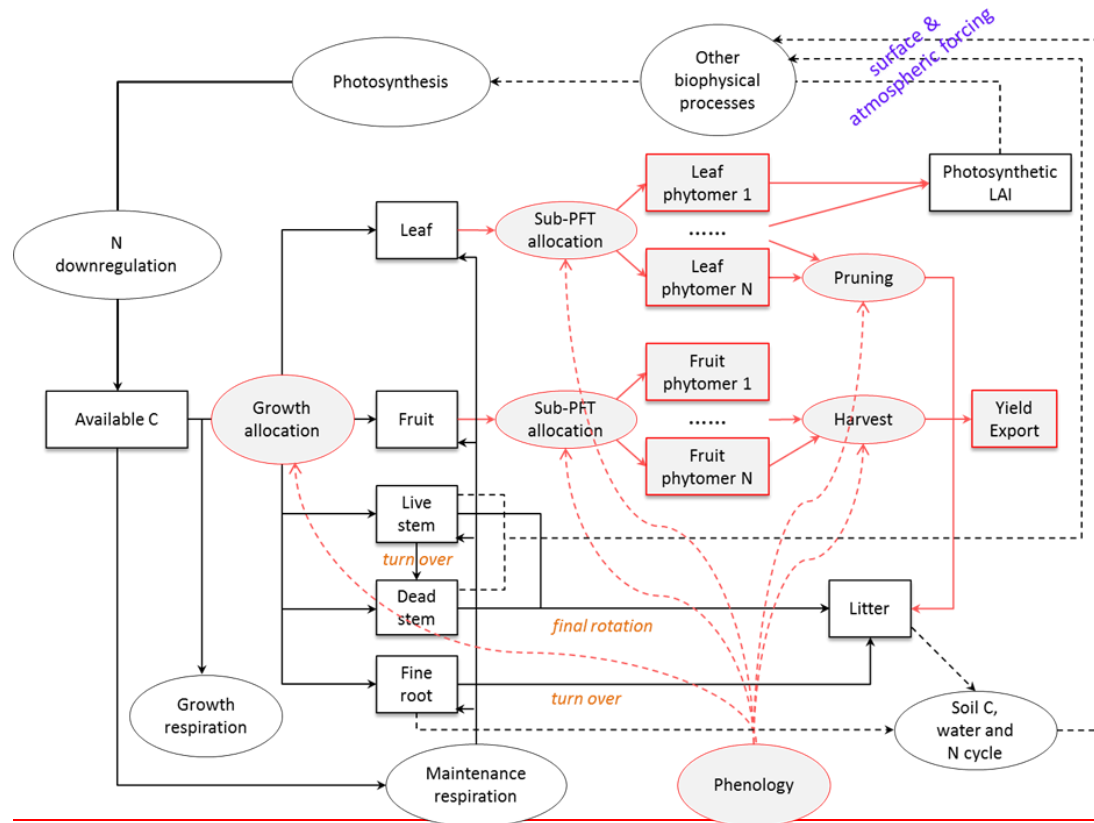
~~The oil palm module is aimed to capture the C and N dynamics within the plantation system from the beginning of its establishment till full vegetative maturity and final rotation (replanting).~~ To be run in a CLM regional or global grid, the age class structure of plantations needs to be taken into account. This can be achieved by setting multiple replicates of the oil palm PFT, each planted at a point of time at a certain grid. As a result, a series of oil palm cohorts developing at different grids could be configured with a transient PFT distribution dataset, which allows for a quantitative analysis of the effects of land-use changes, specifically rainforest to oil palm conversion, on carbon, water and energy fluxes. This will contribute to the land surface modeling community for simulating this structurally unique, economically and ecologically sensitive, and fast expanding oil palm land cover.

## **Acknowledgements:**

This study was funded by the European Commission Erasmus Mundus FONASO Doctorate fellowship. Field trips were partly supported by the Collaborative Research Centre 990 (Ecological and Socioeconomic Functions of Tropical Lowland Rainforest Transformation Systems (Sumatra, Indonesia)) project. We are grateful to Kara Allen (University of Göttingen, Germany), Dr. Bambang Irawan (University of Jambi, Indonesia) and the PTPN-VI plantation in Jambi for providing field data on oil palm. The source code of the post-4.5 version CLM model was provided by Dr. Samuel Levis from National Center for Atmospheric Research (NCAR), Boulder, CO, USA.



Fig. 1. (a) New sub-canopy phytomer structure ~~for oil palm within the CLM framework of~~  
~~CLM-Palm~~.  $P^1$  to  $P^n$  indicate expanded phytomers and  $P^{-1}$  to  $P^{-n}$  at the top indicate  
unexpanded phytomers packed in the bud. Each phytomer has its own phenology, represented  
by different colors corresponding to: (b) the ~~6-phase~~ phytomer phenology: from initiation to  
leaf expansion, to leaf maturity, to fruit-fill, to harvest, to senescence and to pruning.  
Phytomers initiate successively according to the phyllochron (the period in heat unit between  
initiations of two subsequent phytomers). Detailed phenology description is in Supplementary  
materials.



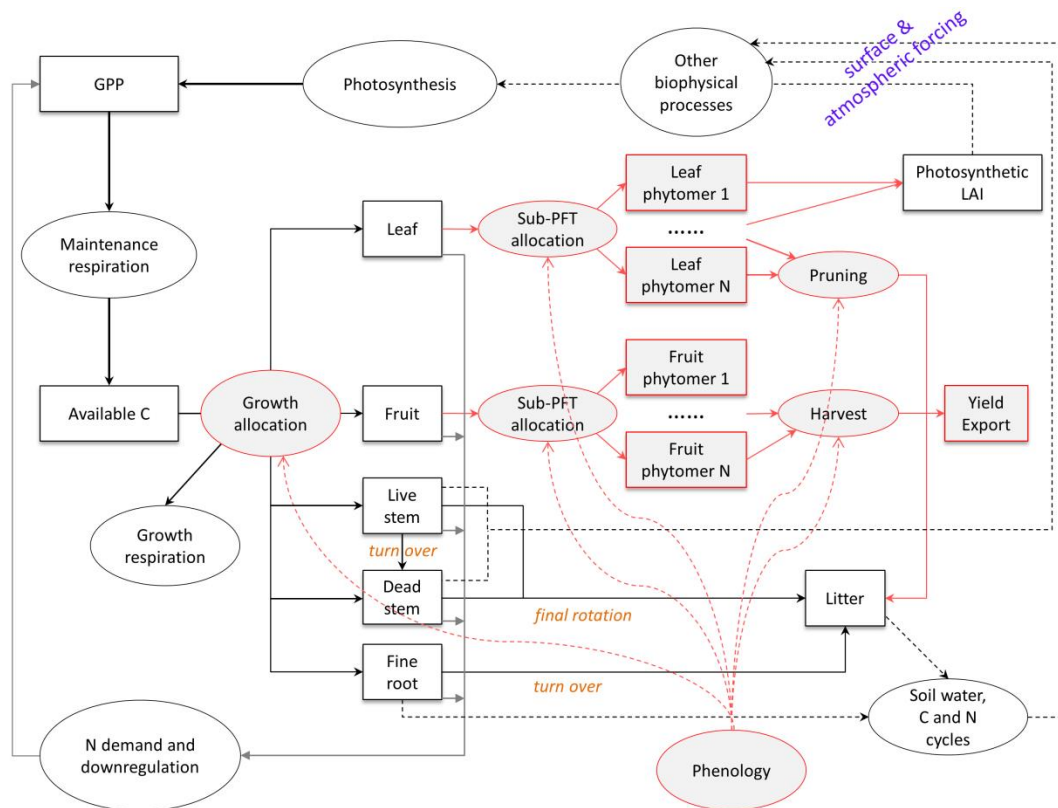


Fig. 2. Original and modified structure and functions for developing CLM-Palm simulating oil palm in the framework of CLM4.5. Original functions from CLM4.5 are represented in black. New functions designed for CLM-Palm the specific oil palm PFT are represented in red, including phenology, allocation, pruning, fruit harvest and export, as well as the sub-canopy structure.



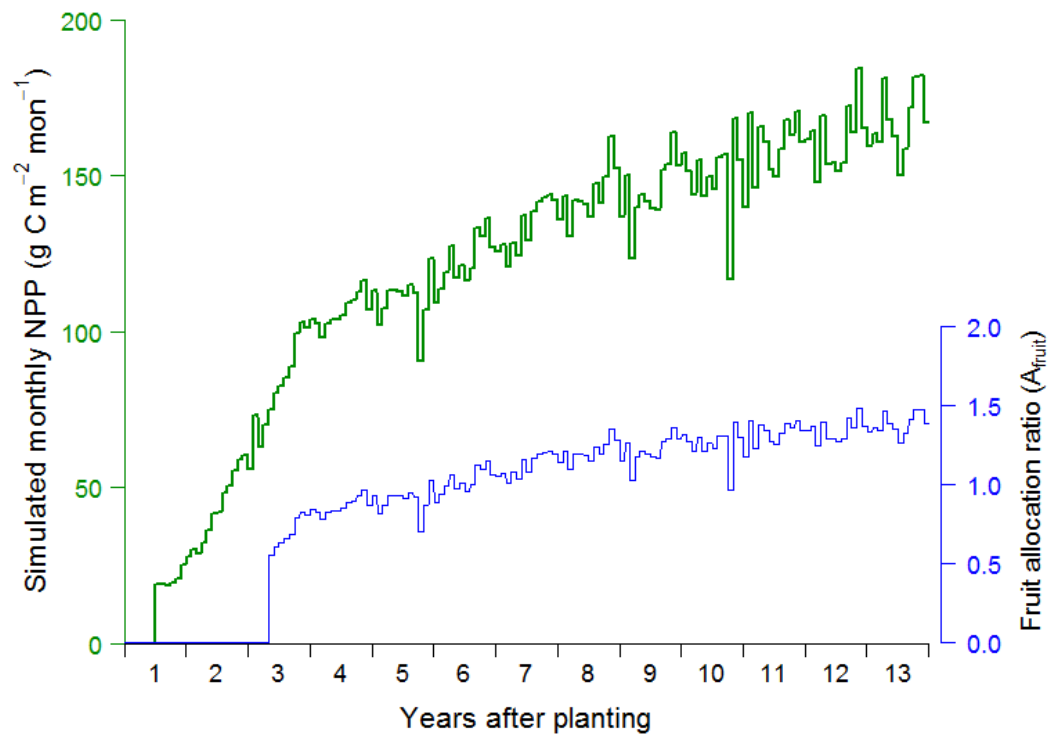


Fig. 3. Time course of reproductive allocation rate (blue line) in relation to monthly NPP from the previous month ( $NPP_{mon}$ , green line) according to Eq. 5.  $A_{fruit}$  is relative to the vegetative unity ( $A_{leaf} + A_{stem} + A_{root} = 1$  and  $0 \leq A_{fruit} \leq 2$ ). The  $NPP_{mon}$  was simulated with calibrated parameters for the PTPN-VI site

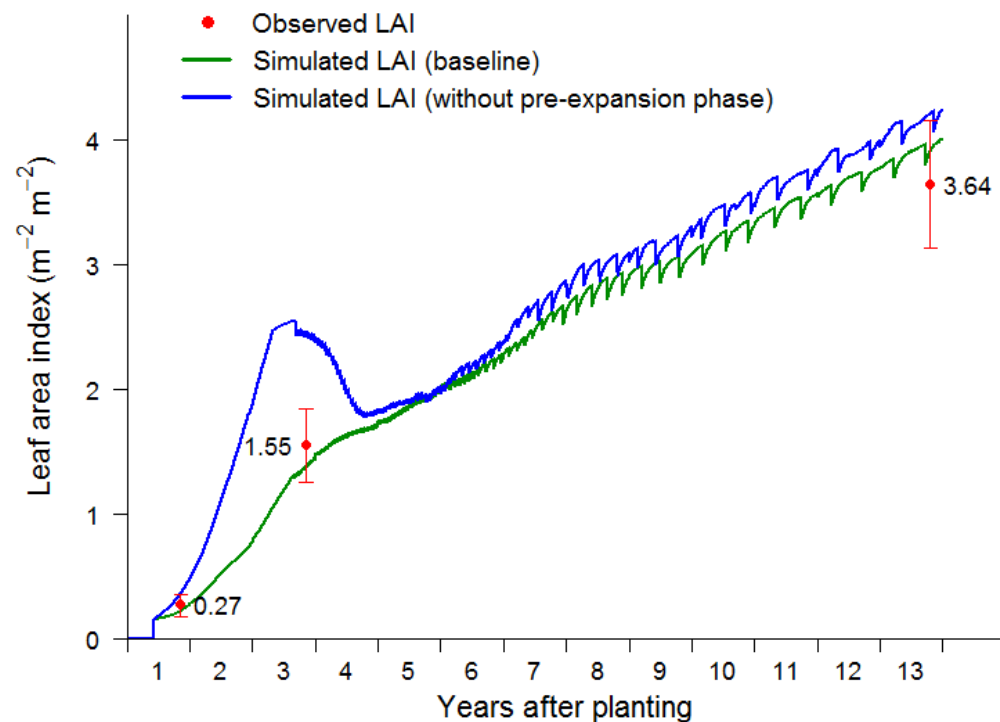
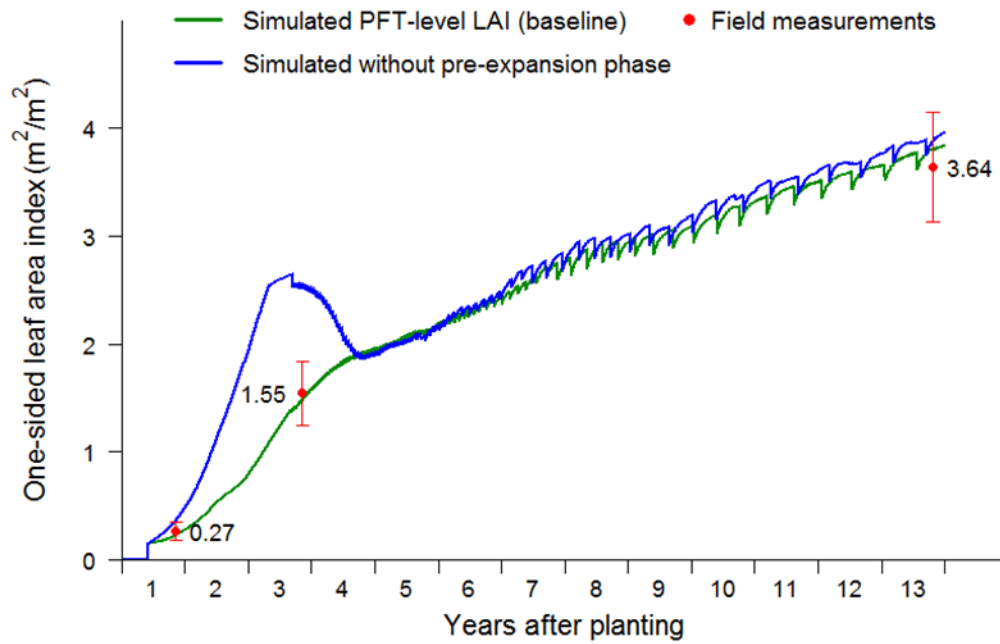
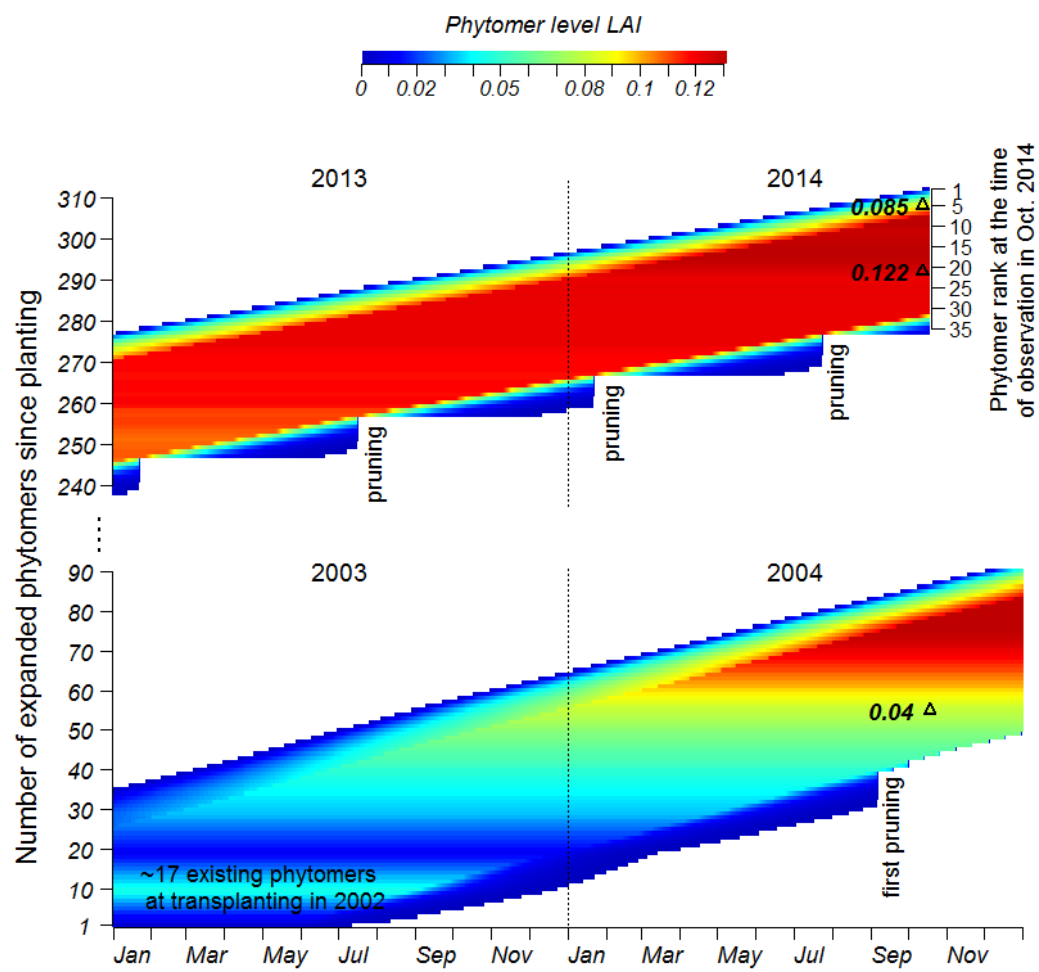


Fig. 34. PFT-level LAI simulated by [CLM-Palmthe-oil-palm-model](#), with and without the pre-expansion growth phase in the phytomer phenology and compared to field measurements used for calibration. The initial sudden increase at year 1 represents transplanting from nursery. The sharp drops mark pruning events.



1122

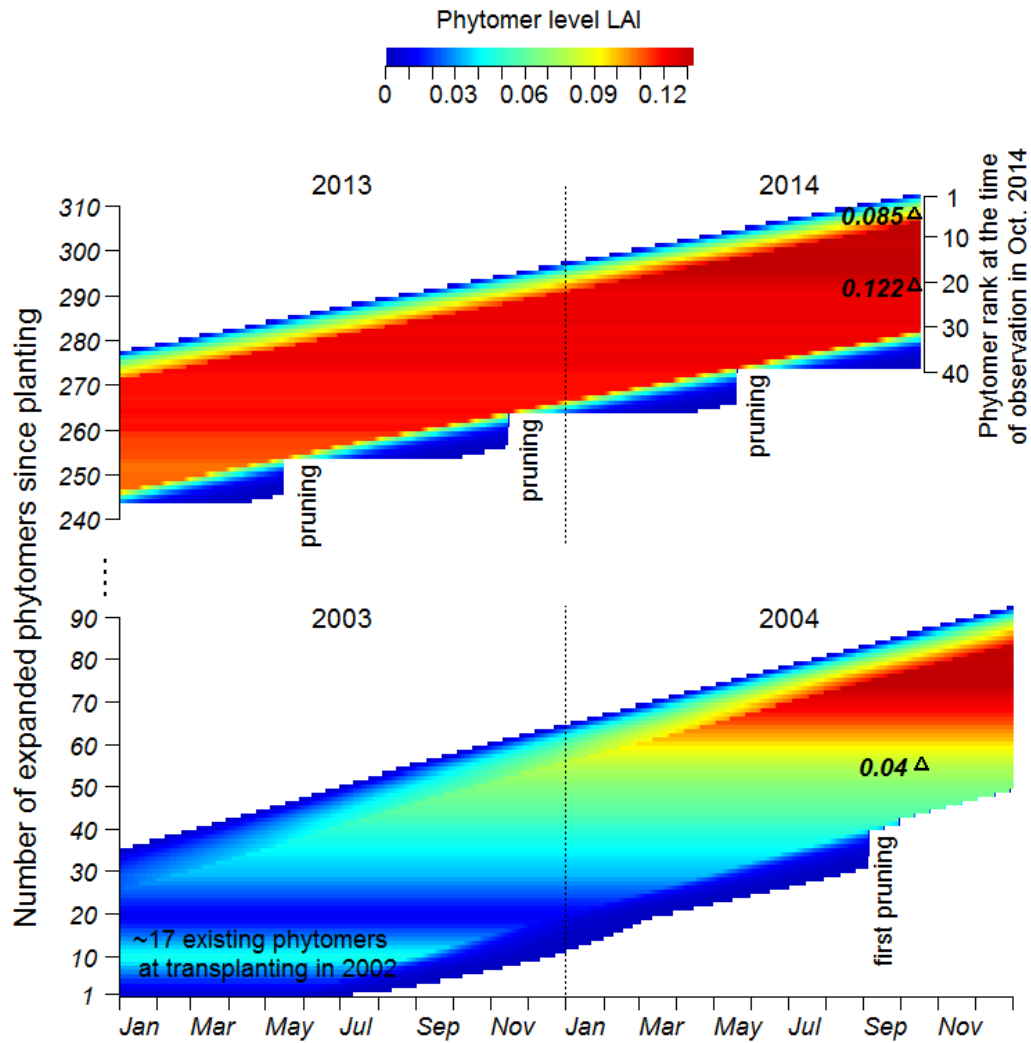


Fig. 45. Simulated phytomer level LAI dynamics (horizontal color bar) compared with field observations (black triangles with measured LAI value). The newly expanded phytomer at a given point of time has a rank of 1. Each horizontal bar represents a part of the life cycle of a phytomer after leaf expansion. Phytomers emerge in sequence and the y-axis gives the total number of phytomers that have expanded since transplanting in the field. Senescent phytomers are pruned. For example, the phytomer ranked at 30 (about to start senescence) at the time of observation in October 2014 was expanded in the beginning of 2013. The one-sided LAIs of two phytomer samples at rank 5 and rank 20 of a mature oil palm in PTPN-VI are within the range of simulated values. The other sample at rank 25 on a young oil palm 2.5 years after transplanting in Pompa Air is slightly lower than the simulated value. Phytomer LAI in the field was estimated by the leaf area divided by 8m×8m, which is the palm planting density.

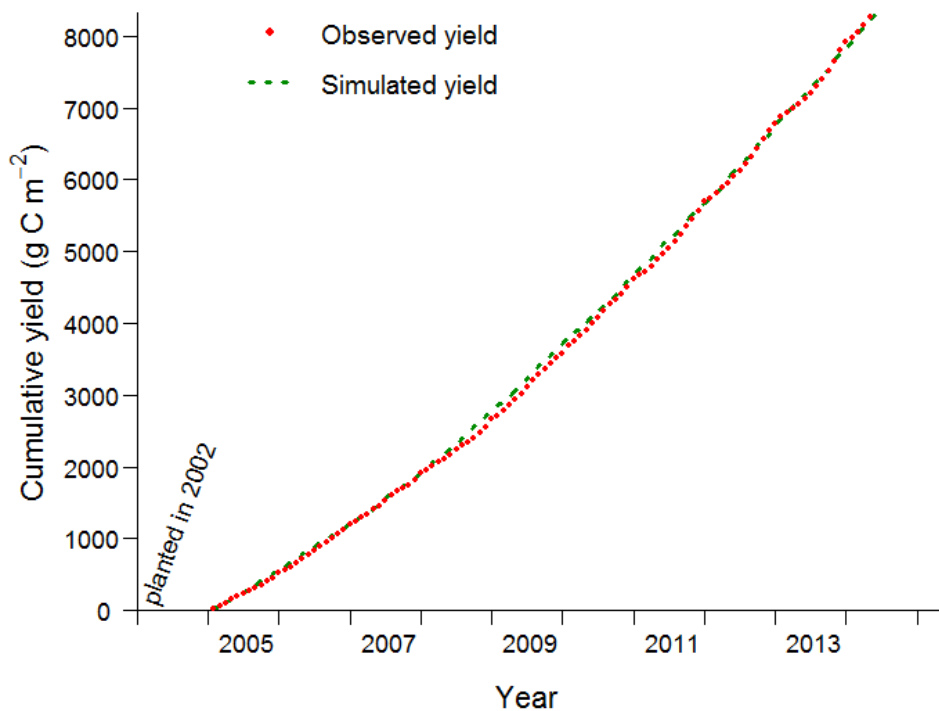
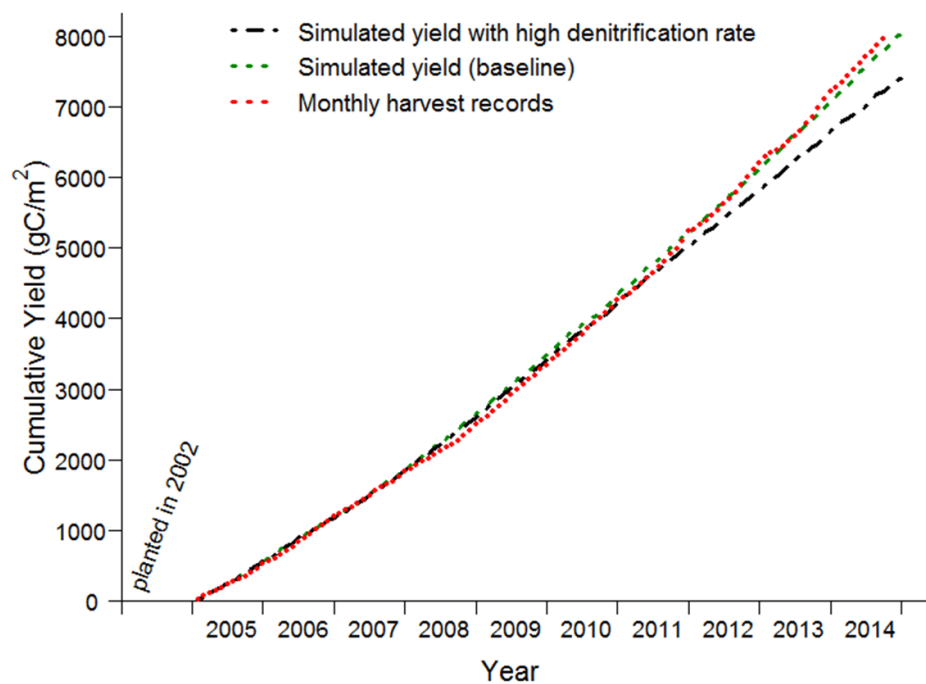
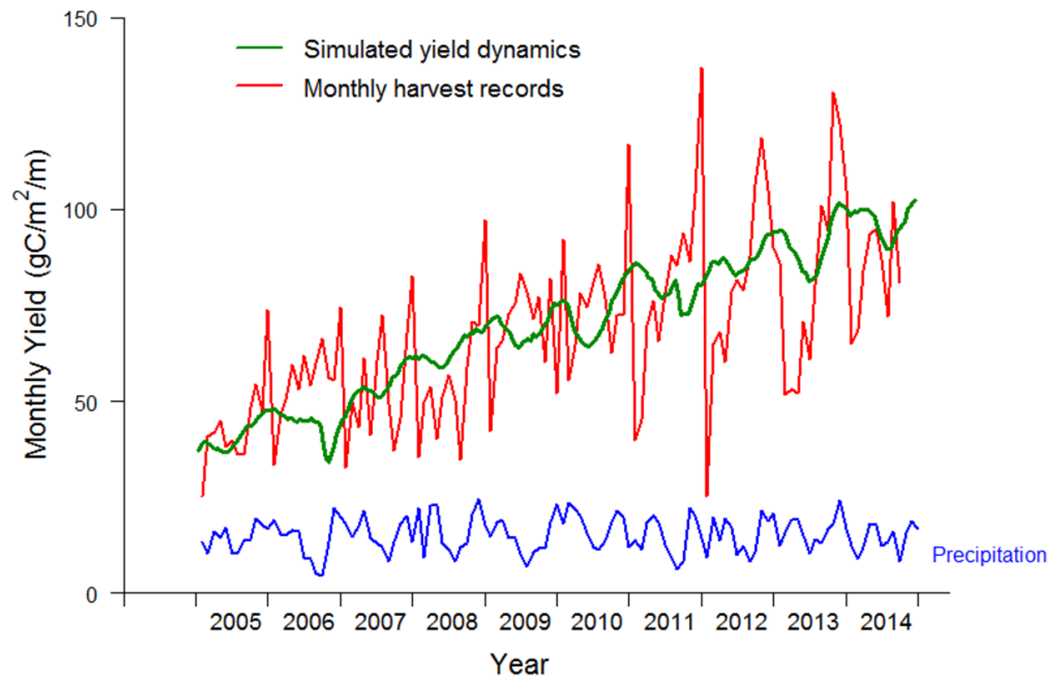


Fig. 56. Simulated PFT-level yield compared with monthly harvest data (2005-2014) from an oil palm plantation (PTPN-VI) in Jambi, Sumatra. CLM-Palm represents multiple harvests from different phytomers (about twice per month). The cumulative harvest amounts throughout time are compared. The oil palm model represents multiple harvests (about twice per month) from different phytomers throughout time. The cumulative harvest amount from

the model matches well with field records (MPE = 4%). If the CLM default high denitrification rate is used, N limitation will bring down final yield.



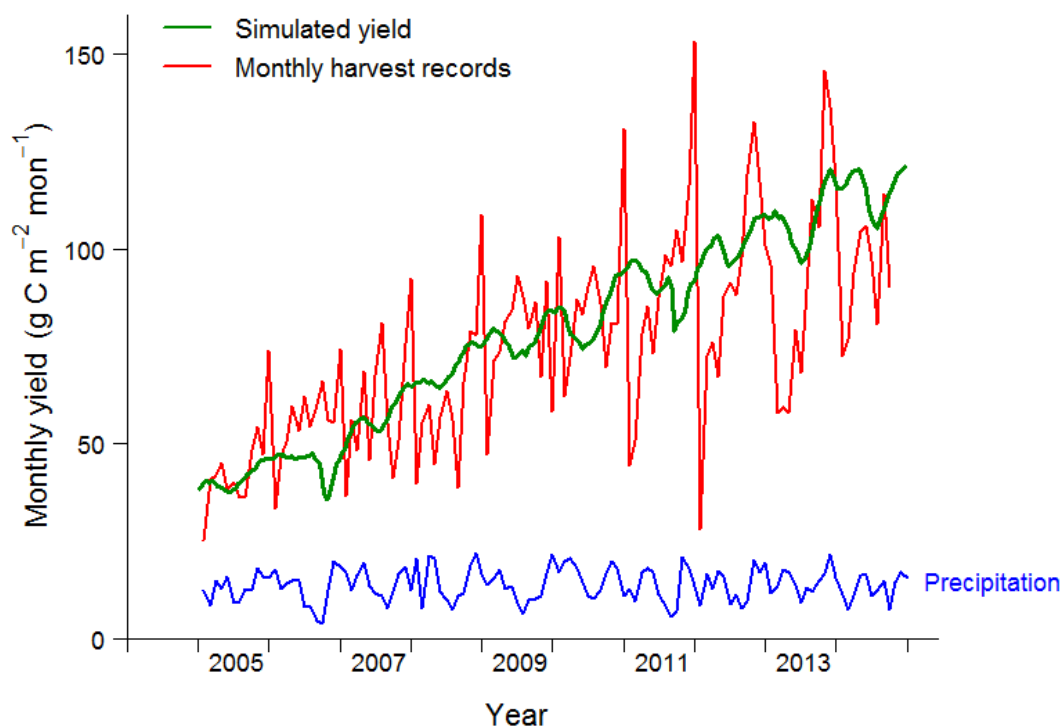
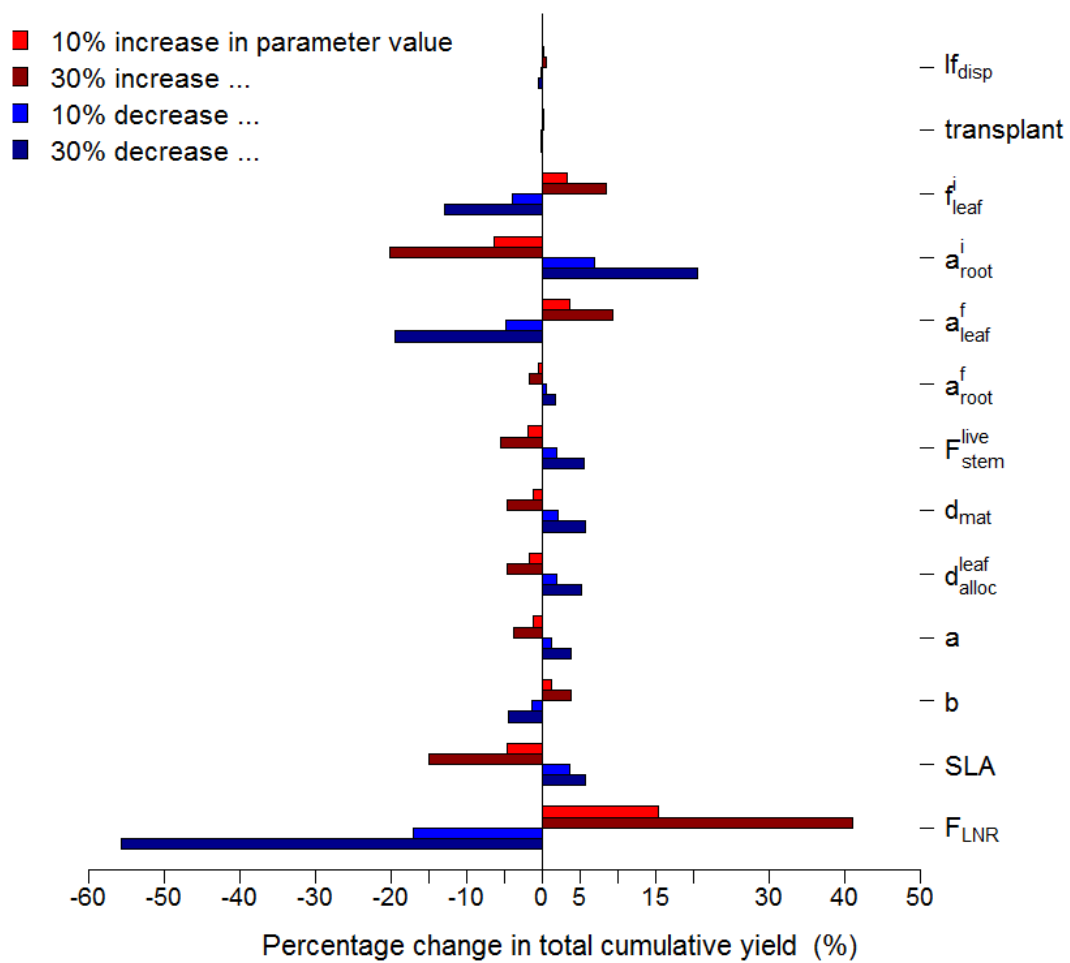


Fig. 67. Simulated and observed monthly yield at PTPN-VI compared with monthly precipitation data (mean: 206 mm per month). The modeled yield outputs are per harvest event (every 15-20 days depending on the phyllochron), while harvest records are the summary of harvest events per month. The model output is thus rescaled to show the monthly trend of yield that matches the mean of harvest records, given that the cumulative yields are almost the same between simulation and observation as shown in Fig. 56.



1155



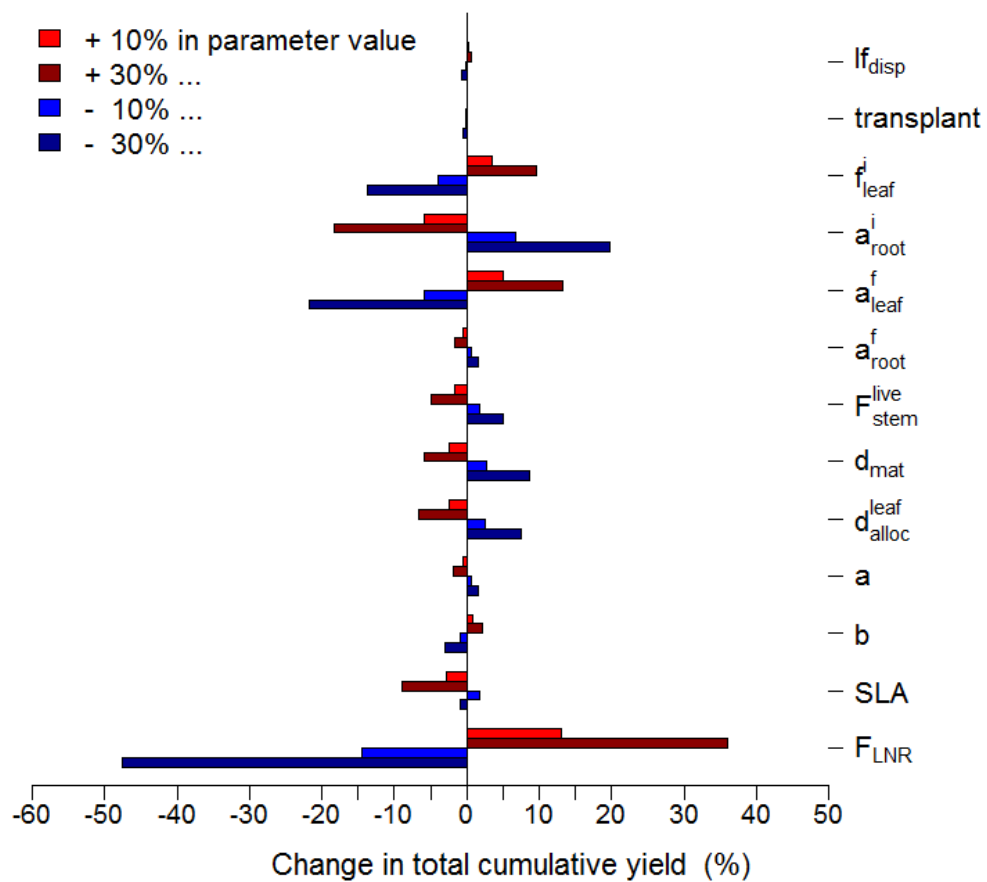


Fig. 78. Sensitivity analysis of key allocation parameters in regard of the cumulative yield at the end of simulation, with two magnitudes of change in the value of a parameter one-by-one while others are hold at the baseline values in Table A2.

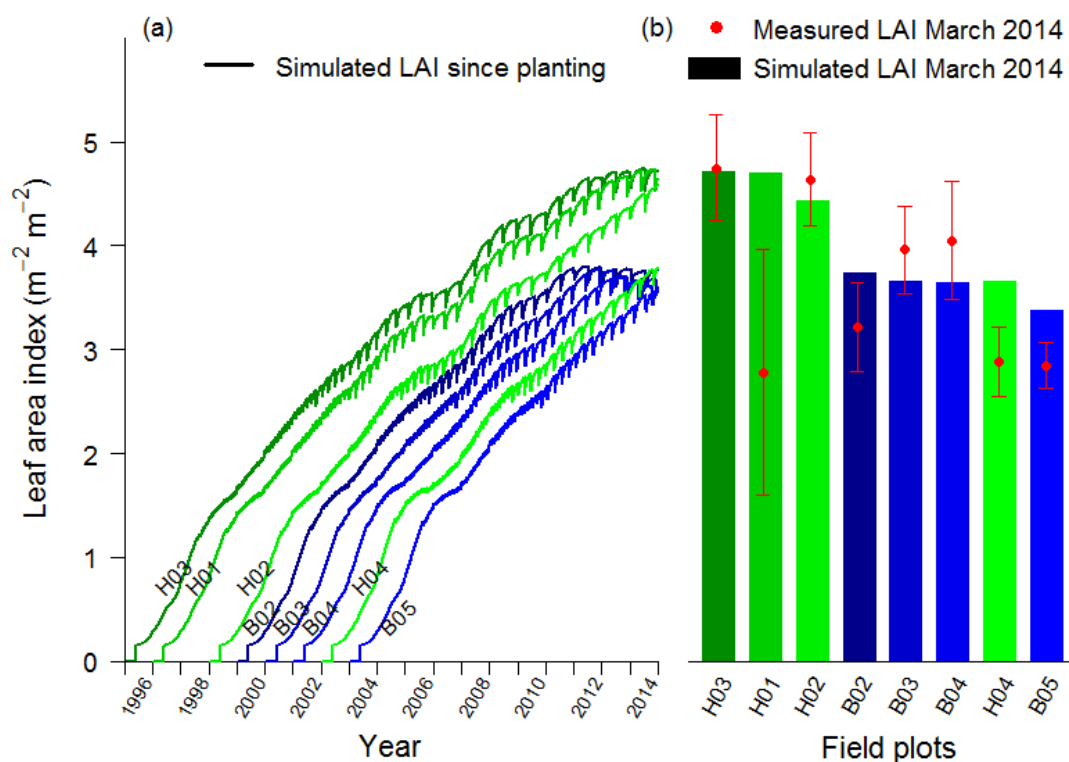
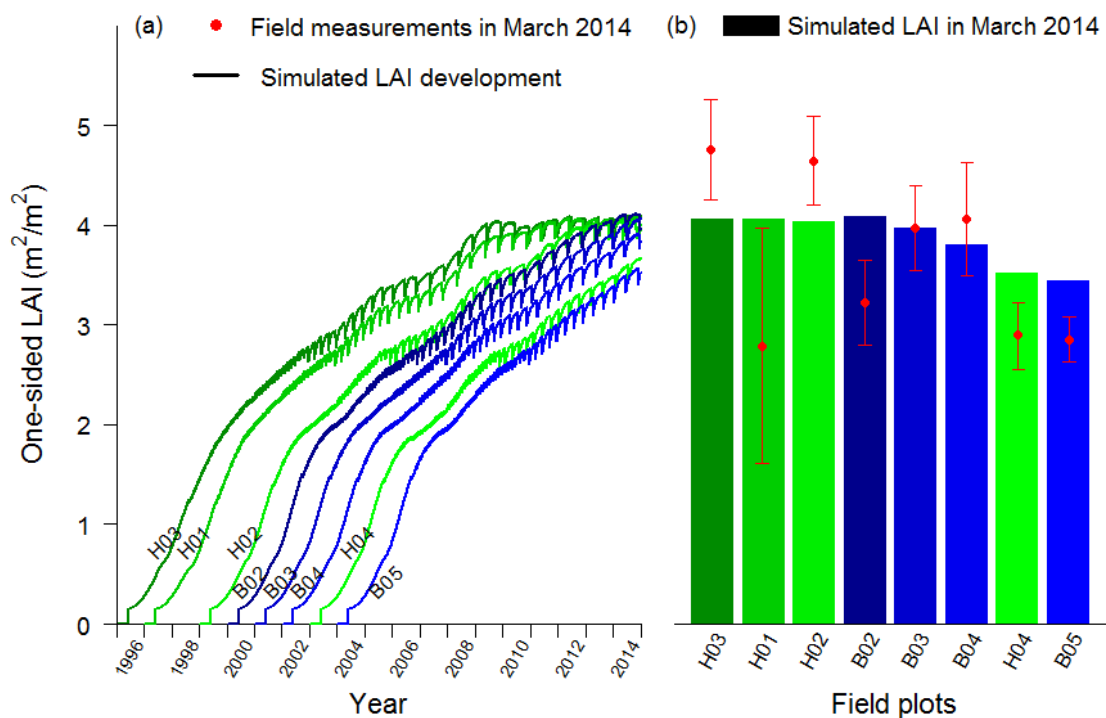


Fig. 89. Validation of LAI with 8 independent oil palm sites (sequence in plantation age) from the Harapan (regular fertilizationH) and Bukit Duabelas (reduced fertilizationB) regions: (a) shows the LAI development of each site simulated by the model since planting; (b) shows the comparison of field measured LAI in 2014 with model.

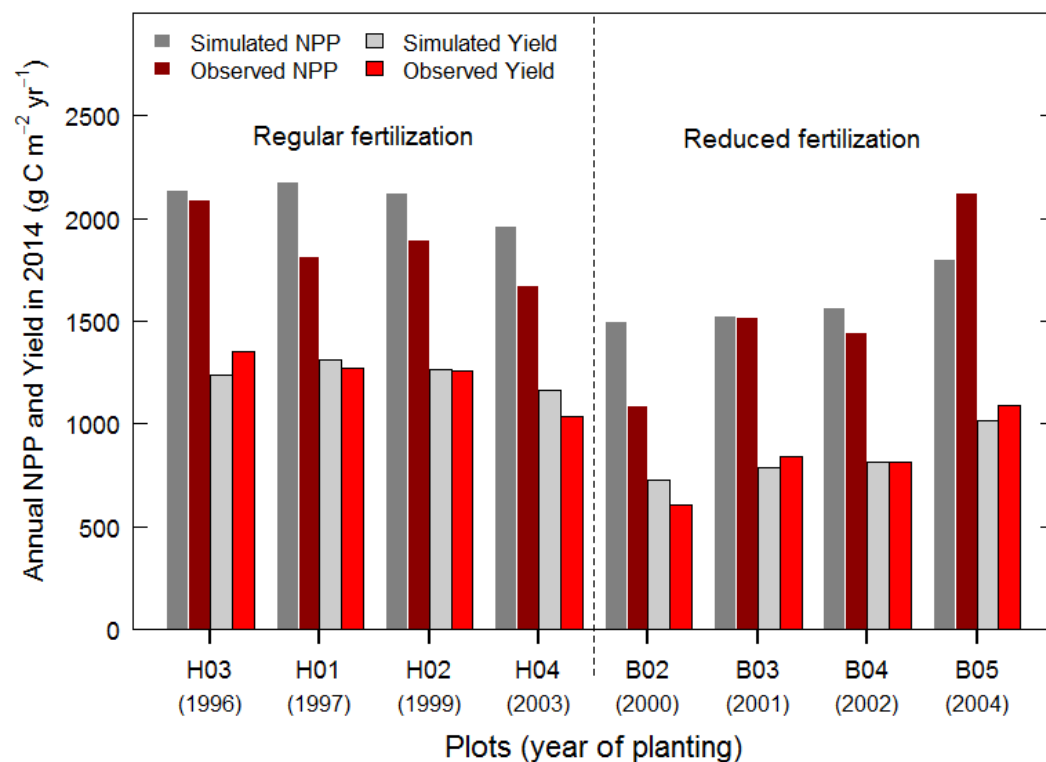
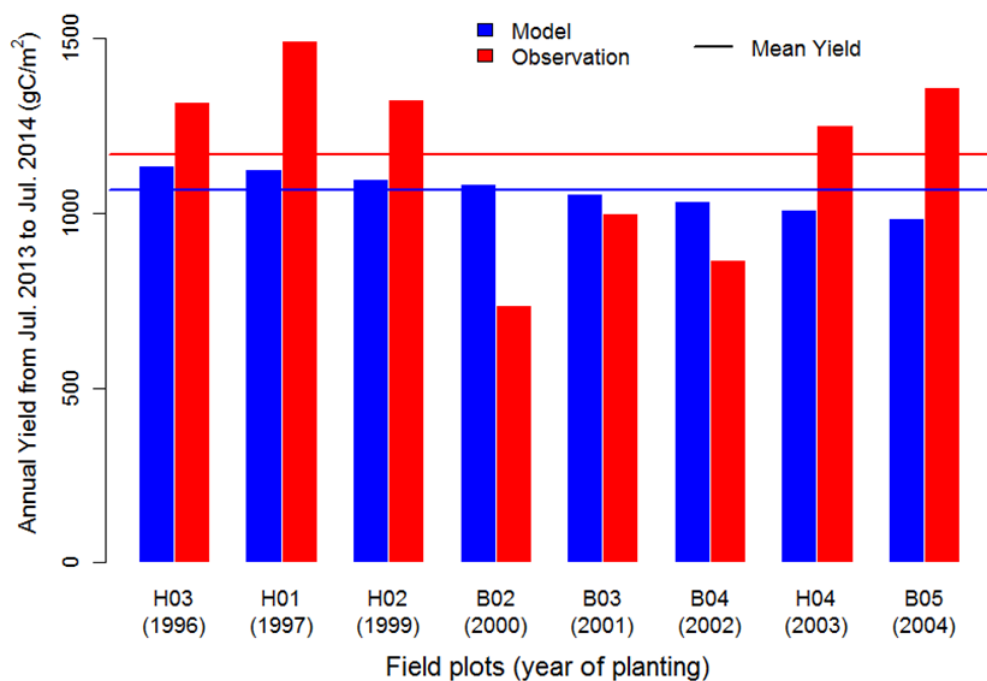


Fig. 910. Validation of yield and NPP with 8 independent oil palm sites from the Harapan (H) and Bukit Duabelas (B) regions with different fertilization treatments. Field data were collected in 2014. The model predicted mean yield matches well with site average but site-to-site variability due to management difference is not reflected by simulation.

1172

**TablesAppendix A**

1173

**Summary of main parameters**

1174

1175

1176

Table A1. Summary of new phenological parameters introduced for ~~the oil palm PFT in~~ the phenology ~~modulesubroutine of CLM-Palm~~. The default values were determined by calibration and with reference to field observations and literatures on oil palm (Combres et al., 2013; Corley and Tinker, 2003; Hormaza et al., 2012; Legros et al., 2009).

Parameter	Default	Min	Max	Explanation (Unit)
$GDD_{init}$	0	0	1500	GDD needed from planting to the first phytomer initiation (°days). Initiation refers to the start of active accumulation of leaf C. A value 0 implies transplanting.
$GDD_{exp}$	1550	0	8000	GDD needed from leaf initiation to start of leaf expansion for each phytomer (pre-expansion) (°days)
$GDD_{L.mat}$	1250	500	1600	GDD needed from start of leaf expansion to leaf maturity for each phytomer (post-expansion) (°days)
$GDD_{F.fill}$	3800	3500	4200	GDD needed from start of leaf expansion to beginning of fruit-fill for each phytomer (°days)
$GDD_{F.mat}$	5200	4500	6500	GDD needed from start of leaf expansion to fruit maturity and harvest for each phytomer (°days)
$GDD_{L.sen}$	6000	5000	8000	GDD needed from start of leaf expansion to beginning of senescence for each phytomer (°days)
$GDD_{end}$	6650	5600	9000	GDD needed from start of leaf expansion to end of senescence for each phytomer (°days)
$GDD_{min}$	7500	6000	10000	GDD needed from planting to the beginning of first fruit-fill (°days)
$Age_{max}$	25	20	30	Maximum plantation age (productive period) from planting to final rotation /replanting (years)
$mxlivenp$	40	30	50	Maximum number of expanded phytomers coexisting on a palm
$phyllochron$	130	100	160	Initial phyllochron (=plastochron): the period in heat unit between the initiations of two successive phytomers. The value increases to 1.5 times, i.e. 195, at 10-year old (°days)

1177

1178 | Table A2. Summary of parameters involved in C and N allocation. The default values were determined by calibration and with reference to field  
1179 | measurements (Kotowska et al., 2015).

Parameter	Defaults	Min	Max	Explanation (Unit)
$*l_{disp}^i$	0.3	0.1	1	Fraction of C and N allocated to the displayed leaf pool
$*transplant$	0.15	0	0.3	Initial total LAI assigned to existing expanded phytomers at transplanting. Value 0 implies planting as seeds.
$f_{leaf}^i$	0.4615	0	1	Initial value of leaf allocation coefficient before the first fruit-fill
$a_{root}^i$	0.3	0	1	Initial value of root allocation coefficient before the first fruit-fill
$a_{leaf}^f$	0.2728	0	1	Final value of leaf allocation coefficient after vegetative maturity
$a_{root}^f$	0.1	0	1	Final value of root allocation coefficient after vegetative maturity
$F_{stem}^{live}$	0.15	0	1	Fraction of new stem allocation that goes to live stem tissues, <u>the rest to metabolically inactive stem tissues</u>
$d_{mat}$	0.56	0.1	1	Factor to control the age when the leaf allocation ratio stabilizes at $a_{leaf}^f$ according to Eq. A54
$d_{alloc}^{leaf}$	0.6	0	5	Factor to control the nonlinear function in Eq. A54. Values < 1 give a convex curve and those > 1 give a concave curve. Value 1 gives a linear function.
$*a$	0.28	0	1	Parameter $a$ for fruit allocation coefficient $A_{fruit}$ in Eq. 25
$*b$	0.0302	0	1	Parameter $b$ for fruit allocation coefficient $A_{fruit}$ in Eq. 25
$PLAI_{max}$	0.165	0.1	0.2	Maximum LAI of a single phytomer ( $m^2 m^{-2}$ )
$SLA$	0.013	0.01	0.015	Specific leaf area ( $m^2 g^{-1} C$ )
$F_{LNR}$	0.07620.1005	0.05	0.1	Fraction of leaf nitrogen in Rubisco enzyme. Used together with $SLA$ to calculate $V_{cmax25}$ ( $g N Rubisco g^{-1} N$ )

1180 | \*New parameters introduced for the oil palm PFT. Others are existing parameters in CLM but mostly are redefined or used in changed context.

Table A3. Other optical, morphological, and physiological parameters for the oil palm PFT.

<u>Parameter</u>	<u>Value</u>	<u>Definition (Unit)</u>	<u>Comments</u>
$CN_{leaf}$	33	Leaf carbon-to-nitrogen ratio ( $g\ C\ g^{-1}\ N$ )	By leaf C:N analysis
$CN_{root}$	42	Root carbon-to-nitrogen ratio ( $g\ C\ g^{-1}\ N$ )	Same as all other PFTs
$CN_{livedwd}$	50	Live stem carbon-to-nitrogen ratio ( $g\ C\ g^{-1}\ N$ )	Same as all other PFTs
$CN_{deadwd}$	500	Dead stem carbon-to-nitrogen ratio ( $g\ C\ g^{-1}\ N$ )	Same as all other PFTs
$CN_{flit}$	60	Leaf litter carbon-to-nitrogen ratio ( $g\ C\ g^{-1}\ N$ )	Same as other tree PFTs
$CN_{fruit}$	75	Fruit carbon-to-nitrogen ratio ( $g\ C\ g^{-1}\ N$ )	Higher than the value 50 for other crops because of high oil content in palm fruit
$r_{vis/nir}^{leaf}$	0.09/0.45	Leaf reflectance in the visible (VIS) or near-infrared (NIR) bands	Values adjusted in-between trees and crops
$r_{vis/nir}^{stem}$	0.16/ 0.39	Stem reflectance in the visible or near-infrared bands	Values adjusted in-between trees and crops
$\tau_{vis/nir}^{leaf}$	0.05/0.25	Leaf transmittance in the visible or near-infrared bands	Values adjusted in-between trees and crops
$\tau_{vis/nir}^{stem}$	0.001/ 0.001	Stem transmittance in the visible or near-infrared bands	Values adjusted in-between trees and crops
$\chi_L$	-0.4	Leaf angle distribution index for radiative transfer (0 = random leaves; 1 = horizontal leaves; -1 = vertical leaves)	Estimated by field observation. In CLM, $-0.4 \leq \chi_L \leq 0.6$
$taper$	50	Ratio of stem height to radius-at-breast-height	Field observation. Used together with <i>stocking</i> and <i>dwood</i> to calculate canopy top and bottom heights.
<i>stocking</i>	150	Number of palms per hectare ( $stems\ ha^{-2}$ )	Field observation. Used to calculate stem area index (SAI) by: $SAI = 0.05 \times LAI \times stocking$ .

1182	<u><math>d_{wood}</math></u>	<u>100000</u>	<u>Wood density (<math>\text{gC m}^{-3}</math>)</u>	<u>Similar as coconut palm (O. Roupsard, personal communication)</u>
	<u><math>R_{z0m}</math></u>	<u>0.05</u>	<u>Ratio of momentum roughness length to canopy top height</u>	<u>T. June, personal communication</u>
	<u><math>R_d</math></u>	<u>0.76</u>	<u>Ratio of displacement height to canopy top height</u>	<u>T. June, personal communication</u>

~~Appendix A (This appendix is merged to main text in section 2.2.1.)~~

~~Allocation equations for the vegetative components before and after fruiting starts:~~

~~1) From leaf emergence to beginning of fruiting~~

$$A_{root} = a_{root}^i - (a_{root}^i - a_{root}^f) \frac{DPP}{Age_{max}}, \quad (\text{Eq. A1})$$

~~where  $\frac{DPP}{Age_{max}} \leq 1$ , and  $DPP$  is the days past planting.~~

$$A_{leaf} = f_{leaf}^i \times (1 - A_{root}) \quad (\text{Eq. A2})$$

$$A_{stem} = 1 - A_{root} - A_{leaf} \quad (\text{Eq. A3})$$

~~2) From beginning of fruiting to maximum age~~

$$A_{root} = a_{root}^i - (a_{root}^i - a_{root}^f) \frac{DPP}{Age_{max}}, \quad (\text{same as A1}) \quad (\text{Eq. A4})$$

$$A_{leaf} = a_{leaf}^2 - (a_{leaf}^2 - a_{leaf}^f) \frac{DPP - DPP_x}{Age_{max} \times d_{mat} - DPP_x} \frac{a_{alloc}^{leaf}}{a_{alloc}^{leaf}}, \quad (\text{Eq. A5})$$

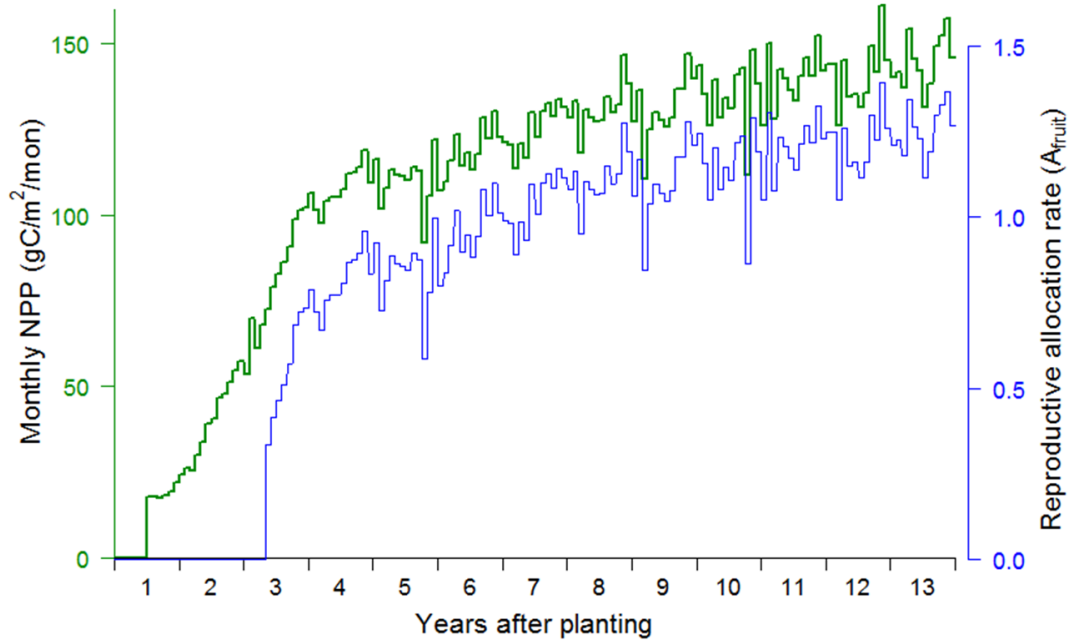
~~where  $a_{leaf}^2$  equals the last value of  $A_{leaf}$  calculated right before fruit fill starts and  $DPP_x$  is~~

~~the days past planting right before fruit fill starts.  $0 \leq \frac{DPP - DPP_x}{Age_{max} \times d_{mat} - DPP_x} \leq 1$ .~~

$$A_{stem} = 1 - A_{root} - A_{leaf}, \quad (\text{same as A3}) \quad (\text{Eq. A6})$$



1200



1201

1202 ~~Fig. A7. Reproductive allocation rate ( $A_{fruit}$ ) as a function of monthly sum of NPP from the~~  
 1203 ~~previous month ( $NPP_{mon}$ ) according to Eq.2 in section 2.2.1.  $A_{fruit}$  is relative to the vegetative~~  
 1204 ~~unity ( $A_{leaf} + A_{stem} + A_{root} = 1$ ).~~

1205 ~~Appendix B (Move to Table A3)~~

1206

1207 ~~Table B1. Other optical, morphological, and physiological parameters for the oil palm PFT.~~

<del>Parameter</del>	<del>Value</del>	<del>Definition (Unit)</del>	<del>Comments</del>
<del><math>CN_{leaf}</math></del>	<del>25</del>	<del>Leaf carbon to nitrogen ratio (<math>g\ C\ g^{-1}\ N</math>)</del>	<del>Same as all other PFTs</del>
<del><math>CN_{root}</math></del>	<del>42</del>	<del>Root carbon to nitrogen ratio (<math>g\ C\ g^{-1}\ N</math>)</del>	<del>Same as all other PFTs</del>
<del><math>CN_{livewd}</math></del>	<del>50</del>	<del>Live stem carbon to nitrogen ratio (<math>g\ C\ g^{-1}\ N</math>)</del>	<del>Same as all other PFTs</del>
<del><math>CN_{deadwd}</math></del>	<del>500</del>	<del>Dead stem carbon to nitrogen ratio (<math>g\ C\ g^{-1}\ N</math>)</del>	<del>Same as all other PFTs</del>
<del><math>CN_{flit}</math></del>	<del>50</del>	<del>Leaf litter carbon to nitrogen ratio (<math>g\ C\ g^{-1}\ N</math>)</del>	<del>Same as all other PFTs</del>
<del><math>CN_{fruit}</math></del>	<del>75</del>	<del>Fruit carbon to nitrogen ratio (<math>g\ C\ g^{-1}\ N</math>)</del>	<del>Higher than the value 50 for other crops because of high oil content in palm seed</del>
<del><math>r_{vis/nir}^{leaf}</math></del>	<del>0.09/0.45</del>	<del>Leaf reflectance in the visible (VIS) or near-infrared (NIR) bands</del>	<del>Values adjusted in between trees and crops</del>
<del><math>r_{vis/nir}^{stem}</math></del>	<del>0.16/0.39</del>	<del>Stem reflectance in the visible or near-infrared bands</del>	<del>Values adjusted in between trees and crops</del>
<del><math>\tau_{vis/nir}^{leaf}</math></del>	<del>0.05/0.25</del>	<del>Leaf transmittance in the visible or near-infrared bands</del>	<del>Values adjusted in between trees and crops</del>
<del><math>\tau_{vis/nir}^{stem}</math></del>	<del>0.001/0.004</del>	<del>Stem transmittance in the visible or near-infrared bands</del>	<del>Values adjusted in between trees and crops</del>
<del><math>\chi_L</math></del>	<del>0.6</del>	<del>Leaf angle index to calculate optical depth of direct beam (from 0 = random leaves to 1 = horizontal leaves; 1 = vertical leaves)</del>	<del>Average leaf angle according to field observation</del>
<del><math>taper</math></del>	<del>50</del>	<del>Ratio of stem height to radius at breast height</del>	<del>Field observation. Used together with <i>stocking</i> and <i>dwood</i> to calculate canopy top and bottom heights.</del>
<del><math>stocking</math></del>	<del>150</del>	<del>Number of palms per hectare (<math>stems\ ha^{-2}</math>)</del>	<del>Field observation. Used to calculate SAI by:</del>

				<del><math>SAI = -0.05 \times LAI \times stocking.</math></del>
	<del><math>d_{wood}</math></del>	<del>100000</del>	<del>Wood density (<math>gC\ m^{-3}</math>)</del>	<del>Similar as coconut palm (O. Roupsard, personal communication)</del>
	<del><math>R_{z0m}</math></del>	<del>0.065</del>	<del>Ratio of momentum roughness length to canopy top height</del>	<del>T. June, personal communication</del>
	<del><math>R_d</math></del>	<del>0.67</del>	<del>Ratio of displacement height to canopy top height</del>	<del>T. June, personal communication</del>
	<del><math>\psi_o</math></del>	<del>-74000</del>	<del>Soil water potential at full stomatal opening (mm)</del>	<del>Same as tree PFTs</del>
	<del><math>\psi_e</math></del>	<del>-275000</del>	<del>Soil water potential at full stomatal closure (mm)</del>	<del>Same as tree PFTs</del>

1208

## References

- Allen, K., Corre, M. D., Tjoa, A., and Veldkamp, E.: Soil nitrogen-cycling responses to conversion of lowland forests to oil palm and rubber plantations in Sumatra, Indonesia, Submitted to PLOS ONE (in review).
- ~~Bilionis, I., Drewniak, B. A., and Constantinescu, E. M.: Crop physiology calibration in CLM, Geoscientific Model Development, 8(4), 1071-1083, 2015.~~
- Bonan, G. B., Levis, S., Kergoat, L., and Oleson, K. W.: Landscapes as patches of plant functional types: An integrated concept for climate and ecosystem models, *Global Biogeochemical Cycles*, 16 (2), 1021-1051, 2002.
- Carlson, K. M., Curran, L. M., Asner, G. P., Pittman, A. M., Trigg, S. N., and Adeney, J. M.: Carbon emissions from forest conversion by Kalimantan oil palm plantations, *Nature Clim. Change*, 3(3), 283–287, doi:10.1038/nclimate1702, 2012.
- Carrasco, L. R., Larrosa, C., Milner-Gulland, E. J., and Edwards, D. P.: A double-edged sword for tropical forests, *Science*, 346(6205), 38-40, 2014.
- Collatz, G. J., Ball, J. T., Griwet, C., and Berry, J. A.: Physiological and environmental regulation of stomatal conductance, photosynthesis and transpiration: a model that includes a laminar boundary layer, *Agricultural and Forest Meteorology*, 54(2), 107-136, 1991.
- Combres, J.-C., Pallas, B., Rouan, L., Mialet-Serra, I., Caliman, J.-P., Braconnier, S., Soulie, J.-C., and Dingkuhn, M.: Simulation of inflorescence dynamics in oil palm and estimation of environment-sensitive phenological phases: a model based analysis, *Functional Plant Biology*, 40(3), 263-279, 2013.
- Corley R. H. V. and Tinker, P. B. (Eds.): *The oil palm*, 4th edition, Blackwell Science, Oxford, 2003.
- Dai, Y., Dickinson, R. E., and Wang, Y. P.: A two-big-leaf model for canopy temperature, photosynthesis, and stomatal conductance, *Journal of Climate*, 17(12), 2281-2299, 2004.
- ~~Dee, D. P., Uppala, S. M., Simmons, A. J., Berrisford, P., Poli, P., Kobayashi, S., ... and Vitart, F.: The ERA-Interim reanalysis: Configuration and performance of the data assimilation system, *Quarterly Journal of the Royal Meteorological Society*, 137(656), 553-597, 2011.~~
- de Pury D. G. G. and Farquhar G. D.: Simple scaling of photosynthesis from leaves to canopies without the errors of big-leaf models. *Plant Cell and Environment*, 20: 537-557, 1997.
- Drewniak, B., Song, J., Prell, J., Kotamarthi, V. R., and Jacob, R.: Modeling agriculture in the community land model, *Geoscientific Model Development*, 6(2), 495-515, doi:10.5194/gmd-6-495-2013, 2013.
- Euler, M., Hoffmann, M. P., Fathoni, Z., and Schwarze, S.: Exploring yield gaps in smallholder oil palm production systems in eastern Sumatra, Indonesia, Submitted to PLOS ONE (in review).
- Farquhar, G. D., von Caemmerer, S. V., and Berry, J. A.: A biochemical model of photosynthetic CO<sub>2</sub> assimilation in leaves of C<sub>3</sub> species, *Planta*, 149(1), 78-90, 1980.
- FAO. FAOSTAT Database, Food and Agriculture Organization of the United Nations, Rome, Italy, available at: <http://faostat.fao.org/site/339/default.aspx> (last access: 17 June 2015), 2013.
- Galloway, J. N., Dentener, F. J., Capone, D. G., Boyer, E. W., Howarth, R. W., Seitzinger, S. P., ... and Vöösmary, C. J.: Nitrogen cycles: past, present, and future, *Biogeochemistry*, 70(2), 153-226, 2004.
- Georgescu, M., Lobell, D. B., and Field, C. B.: Direct climate effects of perennial bioenergy crops in the United States, *Proceedings of the National Academy of Sciences*, 108(11), 4307-4312, 2011.
- Goh K. J.: Climatic requirements of the oil palm for high yields, in: *Managing oil palm for high yields: agronomic principles*, Goh K.J. (Eds.), pp. 1–17, Malaysian Soc. Soil Sci. and Param Agric. Surveys, Kuala Lumpur, 2000.

- Guillaume, T., Damris, M., and Kuzyakov, Y.: Losses of soil carbon by converting tropical forest to plantations: erosion and decomposition estimated by  $\delta^{13}\text{C}$ , *Global change biology*, 21, 3548–3560, doi: 10.1111/gcb.12907, 2015.
- Gunarso, P., Hartoyo, M. E., Agus, F., and Killeen, T. J.: Oil Palm and Land Use Change in Indonesia, Malaysia, and Papua New Guinea. In: Killeen T, Goon J, editors. *Reports from the Science Panel of the Second GHG Working Group of the Roundtable for Sustainable Palm Oil (RSPO)*. Kuala Lumpur, 2013.
- Hallé F., Oldeman, R. A. A. and Tomlinson, P. B.: Tropical trees and forests. An architectural analysis. Springer-Verlag, Berlin, 441 pp., 1978.
- Hijmans, R. J., Cameron, S. E., Parra, J. L., Jones, P. G., and Jarvis, A.: Very high resolution interpolated climate surfaces for global land areas, *International journal of climatology*, 25(15), 1965–1978, 2005.
- Hoffmann, M. P., Vera, A. C., Van Wijk, M. T., Giller, K. E., Oberthür, T., Donough, C., and Whitbread, A. M.: Simulating potential growth and yield of oil palm (*Elaeis guineensis*) with PALMSIM: Model description, evaluation and application, *Agricultural Systems*, 131, 1–10, 2014.
- Hormaza, P., Fuquen, E. M., and Romero, H. M.: Phenology of the oil palm interspecific hybrid *Elaeis oleifera*  $\times$  *Elaeis guineensis*, *Scientia Agricola*, 69(4), 275–280, 2012.
- Huth, N. I., Banabas, M., Nelson, P. N., and Webb, M.: Development of an oil palm cropping systems model: lessons learned and future directions, *Environ. Modell. Softw.*, 62, 411–419, doi:10.1016/j.envsoft.2014.06.021, 2014.
- Jin, J. M. and Miller, N. L.: Regional simulations to quantify land use change and irrigation impacts on hydroclimate in the California Central Valley, *Theoretical and Applied Climatology*, 104, 429–442, 2011.
- Koh, L. P. and Ghazoul, J.: Spatially explicit scenario analysis for reconciling agricultural expansion, forest protection, and carbon conservation in Indonesia, *P. Natl. Acad. Sci. USA*, 107, 11140–11144, doi: 10.1073/pnas.1000530107, 2010.
- Kotowska, M. M., Leuschner, C., Antono, T., Meriem, S., and Hertel, D.: Quantifying aboveand belowground biomass carbon loss with forest conversion in tropical lowlands of Sumatra (Indonesia), *Global Change Biol.*, accepted, doi: 10.1111/gcb.12979, 2015.
- Koven, C. D., Riley, W. J., Subin, Z. M., Tang, J. Y., Torn, M. S., Collins, W. D., Bonan, G. B., Lawrence, D. M., and Swenson, S. C.: The effect of vertically resolved soil biogeochemistry and alternate soil C and N models on C dynamics of CLM4, *Biogeosciences*, 10(11), 7109–7131, doi:10.5194/bg-10-7109-2013, 2013.
- Kucharik, C. J., and Brye, K. R.: Integrated Biosphere Simulator (IBIS) yield and nitrate loss predictions for Wisconsin maize receiving varied amounts of nitrogen fertilizer, *Journal of Environmental Quality* 32, 247–268, 2003.
- Legros, S., Mialet-Serra, I., Caliman, J. P., Siregar, F. A., Clement-Vidal A., and Dingkuhn, M.: Phenology and growth adjustments of oil palm (*Elaeis guineensis*) to photoperiod and climate variability, *Annals of Botany* 104, 1171–1182. doi:10.1093/aob/mcp214, 2009.
- Levis, S., Bonan, G., Kluzek, E., Thornton, P., Jones, A., Sacks, W., and Kucharik, C.: Interactive crop management in the Community Earth System Model (CESM1): Seasonal influences on land-atmosphere fluxes, *J. Climate*, 25, 4839–4859, DOI:10.1175/JCLI-D-11-00446.1., 2012.
- Luyssaert, S., Schulze, E. D., Börner, A., Knohl, A., Hessenmöller, D., Law, B. E., Ciais, P., and Grace, J.: Old-growth forests as global carbon sinks, *Nature*, 455(7210), 213–215, 2008.
- Miettinen, J., Shi, C. H. and Liew, S. C.: Deforestation rates in insular Southeast Asia between 2000 and 2010, *Global Change Biology*, 17, 2261–2270, 2011.
- Navarro, M. N. V., Jourdan, C., Sileye, T., Braconnier, S., Mialet-Serra, I., Saint-Andre, L., ... and Rouspard, O.: Fruit development, not GPP, drives seasonal variation in NPP in a tropical palm plantation, *Tree physiology*, 28(11), 1661–1674, 2008.

- Norman, J. M.: Modeling the complete crop canopy, in *Modification of the Aerial Environment of Plants*, edited by Barfield, B. J. and Gerber, J. F., pp. 249–277, Am. Soc. Agric. Eng., St. Joseph, MI., 1979.
- Oleson, K. W., Bonan, G. B., Levis, S., and Vertenstein, M.: Effects of land use change on North American climate: impact of surface datasets and model biogeophysics, *Climate Dynamics*, 23, 117–132, 2004.
- Oleson, K., Lawrence, D., Bonan, G., Drewniak, B., Huang, M., Koven, C., Levis, S., Li, F., Riley, W., Subin, Z., Swenson, S., Thornton, P., Bozbiyik, A., Fisher, R., Heald, C., Kluzek, E., Lamarque, J.-F., Lawrence, P., Leung, L., Lipscomb, W., Muszala, S., Ricciuto, D., Sacks, W., Sun, Y., Tang, J., and Yang, Z.-L.: Technical description of version 4.5 of the Community Land Model (CLM), National Center for Atmospheric Research, Boulder, Colorado, USA, 420 pp., doi:10.5065/D6RR1W7M, 2013.
- Roupsard, O., Dauzat, J., Nouvellon, Y., Deveau, A., Feintrenie, L., Saint-André L., ... and Bouillet, J. P.: Cross-validating sun-shade and 3D models of light absorption by a tree-crop canopy, *Agricultural and Forest Meteorology*, 148(4), 549–564, 2008.
- Ryan, M. G.: A simple method for estimating gross carbon budgets for vegetation in forest ecosystems, *Tree Phys.*, 9, 255–266, 1991.
- Ryu, Y., Baldocchi, D. D., Kobayashi, H., van Ingen, C., Li, J., Black, T. A., Beringer, J., van Gorsel, E., Knohl, A., Law, B. E., and Roupsard, O. Integration of MODIS land and atmosphere products with a coupled-process model to estimate gross primary productivity and evapotranspiration from 1 km to global scales, *Global Biogeochemical Cycles*, 25, GB4017, doi:10.1029/2011GB004053., 2011.
- Sellers, P. J.: Canopy reflectance, photosynthesis and transpiration, *Int. J. Remote Sens.*, 6, 1335–1372, 1985.
- Sellers, P. J., Randall, D. A., Collatz, G. J., Berry, J. A., Field, C. B., Dazlich, D. A., ... and Bounoua, L.: A revised land surface parameterization (SiB2) for atmospheric GCMs. Part I: Model formulation, *Journal of climate*, 9(4), 676–705, 1996.
- Tang, J. Y., Riley, W. J., Koven, C. D., and Subin, Z. M.: CLM4-BeTR, a generic biogeochemical transport and reaction module for CLM4: model development, evaluation, and application, *Geosci. Model Dev.*, 6, 127–140. doi:10.5194/gmd-6-127-2013, 2013.
- van Kraalingen, D. W. G., Breure, C. J., and Spitters, C. J. T.: Simulation of oil palm growth and yield, *Agricultural and forest meteorology*, 46(3), 227–244, 1989.
- Veldkamp, E., and Keller, M.: Nitrogen oxide emissions from a banana plantation in the humid tropics, *Journal of Geophysical Research: Atmospheres* (1984–2012), 102(D13), 15889–15898, 1997.
- Viovy, N.: CRUNCEP dataset: <http://dods.extra.cea.fr/data/p529viov/cruncep/readme.htm> (last access: 14 May 2015), 2011.
- von Uexküll, H., Henson, I. E., and Fairhurst, T.: Canopy management to optimize yield, in: *The Oil Palm – e Management for Large and Sustainable Yields*, Fairhurst, T., and Härdter, R. (Eds.), Potash & Phosphate Institute of Canada, Potash & Phosphate Institute, International Potash Institute, Singapore, pp. 163–180, 2003.
- White, M. A., Thornton, P. E., and Running, S. W.: A continental phenology model for monitoring vegetation responses to interannual climatic variability, *Global Biogeochem. Cycles*, 11, 217–234, 1997.